Applied Water Science (2024) 14:214
https://doi.org/10.1007/s13201-024-02278-0

ORIGINAL ARTICLE

Cumulative effects of natural and anthropogenic processes on groundwater chemistry of a small karst island—case study of Vis (Croatia)

Matko Patekar[1] · **Maja Briški**[1] · **Josip Terzić**[1] · **Zoran Nakić**[2] · **Staša Borović**[1]

Received: 24 May 2024 / Accepted: 28 August 2024

Abstract
Many coastal and island communities depend on groundwater as the only source of freshwater, making it an invaluable resource. In the Mediterranean region, groundwater resources are highly vulnerable to natural and anthropogenic pressures, such as overexploitation, climate change, seasonal variations in precipitation, and seawater intrusion. Hence, an understanding of hydrogeological processes and groundwater chemistry is a basis for the sustainable management of coastal and island groundwater resources. Vis, a small and remote karst island in the Adriatic Sea, exhibits peculiar geological and hydrogeological settings, resulting in the island's autonomous water supply. The current pumping capacity (maximum of 42 l/s) meets most of the demand, but intensive summer tourism and climate change exert high stress on groundwater resources during the dry season. Consequently, in the last decade, occasional reductions for consumers occurred. Monitoring of in situ physicochemical parameters and groundwater sampling for chemical and isotopic analyses were conducted from 2020 to 2023 at deep borewells, shallow dug wells, and springs. Hydrochemical interpretation indicated that groundwater chemistry was affected primarily by carbonate and sulfate rock dissolution, mixing with seawater, reverse ion exchange, and dedolomitization. The majority of groundwater samples exhibit Ca–HCO_3 hydrochemical facies, followed by Na–Cl and mixed facies. The low percentage of seawater in the mixture indicated that seawater intrusion is not too extensive even during prolonged dry periods, implying a favorable hydrostatic regime with relatively small but sufficient groundwater reserves of the island's aquifers, although the investigated period was characterized by significantly lower precipitation with respect to the 30-year average.

Keywords Hydrogeology · Island · Karst · Groundwater chemistry · Seawater intrusion

Introduction

Karst rocks are among the most important aquifers in the world, providing groundwater resources for almost a quarter of the global population (Ford and Williams 2007). Karst aquifers are significantly different compared to aquifers with intergranular porosity since the process of carbonate rock dissolution (i.e., karstification) results in heterogeneous and anisotropic distribution of hydrogeological properties (Goldscheider and Andreo 2007), posing a significant challenge for the investigation, utilization, and management of groundwater resources. Such heterogeneity and anisotropy are often reflected in the hydrodynamic characteristics of springs and discharge zones, as well as the chemical and physicochemical characteristics of the groundwater. In the Mediterranean region, where karst groundwater resources are highly vulnerable, limited, and unevenly distributed, sustainable groundwater management remains one of the critical environmental challenges (García-Ruiz et al. 2011). Climate change, overexploitation, improper land use, user conflicts, and seawater intrusions are the most common drivers of the degradation of groundwater quality and availability (Cudennec et al. 2007; Antonellini et al. 2008; Mongelli et al. 2013; Argamassila et al. 2017; Leduc et al. 2017; Massuel and Riaux 2017). In particular, the

✉ Staša Borović
sborovic@hgi-cgs.hr

[1] Department of Hydrogeology and Engineering Geology, Croatian Geological Survey, Sachsova 2, 10000 Zagreb, Croatia

[2] Faculty of Mining, Geology and Petroleum Engineering, Department of Geology and Geological Engineering, University of Zagreb, Pierottijeva 6, 10000 Zagreb, Croatia

Published online: 09 September 2024

Mediterranean region is often regarded as a hot spot of climate change, with a predicted increase in mean annual air temperature of 3.5–5.5 °C until the end of the century (Branković et al. 2013) and an increase in precipitation variability with a negative influence on water balance (Aguilera and Murillo 2009). Moreover, several studies reported that global warming is already progressively increasing the frequency, intensity, and duration of drought events in the Mediterranean region (Bisselink et al. 2018; Samaniego et al. 2018). In addition, environmental challenges are aggravated by rising anthropic pressure and high population density, with the population drastically increasing during the dry summer tourist season (Tramblay et al. 2020).

Among 79 islands and 525 islets in the Croatian part of the Adriatic Sea (Duplančić Leder et al. 2004), only several have completely autonomous water supply from karst aquifers, freshwater lenses, or freshwater lakes and marshes, whereas the majority are connected to the water supply systems on the mainland (Borović et al. 2019). The most significant problem regarding groundwater utilization on Croatian islands is seawater intrusion. Seawater intrusion and consequent groundwater salinization are common processes affecting many coastal and island aquifers and are often caused by a combination of human and natural factors (Kim et al. 2003; Ghabayen et al. 2006; Behera et al. 2019). Croatian islands are predominantly composed of karstified carbonate rocks (Vlahović et al. 2005) and seawater intrusion is imposed by (i) small surface area and low relief of the islands, resulting in small catchments and low hydraulic gradients, (ii) intense fracturing and karstification with a karst base level below the present sea level, resulting in high permeability of the rock mass and preferential seawater intrusion through karstic conduits, and (iii) climate of the area characterized by relatively low precipitation and high evapotranspiration (Terzić et al. 2010).

Understanding groundwater hydrochemistry and related hydrogeological processes is one of the critical elements in achieving efficient and sustainable management of groundwater resources, particularly in coastal and island areas (Wali 2020; Hamma et al. 2024). The research presented in this paper aims to assess groundwater chemistry and the most significant hydrogeological processes on the island of Vis, a small and remote island located far from the Croatian mainland, in the central part of the Adriatic Sea. The island is specific in terms of having an autonomous water supply from a karst aquifer, with several natural springs that fostered the establishment of prehistoric settlements, as well as Greek and Roman colonies since the fourth century B.C. (Novak 1940). Such favorable hydrogeological conditions result from peculiar geological settings and structures, where diverse lithologies including karstified carbonates, volcanic rocks, evaporites, and clastic deposits intertwine on a relatively small area. The island's groundwater resources sustain most of the demand, but intensive summer tourism and climate change exert high stress on groundwater resources during the dry season. Consequently, in the last decades, occasional reductions for consumers occurred.

This research aims to investigate the most significant processes that influence groundwater chemistry on the island of Vis by utilizing the results from four years of continuous field and laboratory investigations. Understanding the occurrence and characteristics of local hydrogeological processes represents a scientific challenge and has very important practical implications for managing local groundwater resources. The results of this research will foster further development of sustainable groundwater management on the island, including the potential increase of pumping quantity (e.g., new wells at existing water supply site or at prospective areas), accompanied by the establishment of early warning system for seawater intrusion, managed aquifer recharge, and small desalination plant. This research and its methodology, motivated by both scientific interest and social need, could be applied in other coastal and island areas facing similar hydrogeological or hydrological issues and potential degradation of groundwater quality and quantity due to overexploitation, seawater intrusion or climate change.

Study area

The island of Vis is located in the central part of the Adriatic Sea, approximately 43 km west of the Croatian mainland (Fig. 1). The island covers 89.7 km^2 and has approximately 3300 inhabitants (CBS 2021), predominantly living in the towns of Vis and Komiža, while the minor part lives in scattered settlements in the island's interior. The local economy primarily relies on agriculture and fishing, and the island is a popular destination for summer tourism. Morphologically, the island consists of three hilly chains elongated in roughly E–W direction, with northern and southern valleys between them. The latter is more prominent, hosting karst poljes (large flat plains in karstic terrains), where significant agricultural and economic activity occurs (Krklec et al. 2015). The highest peak is Hum (587 m a.s.l.), in the western part of the island. The island is mostly covered by dense Mediterranean vegetation (maquis shrubland), coniferous forests, and agricultural areas (olive groves and vineyards, vegetable gardens and orchards, and pasture).

The climate is Mediterranean type (Csa) with dry and hot summers (Gajić-Čapka et al. 2008; Krklec et al. 2012). During the last thirty years, the mean annual air temperature was 17.2 °C and the mean annual precipitation was 745 mm (minimum 410 mm/a, maximum 1269 mm/a;

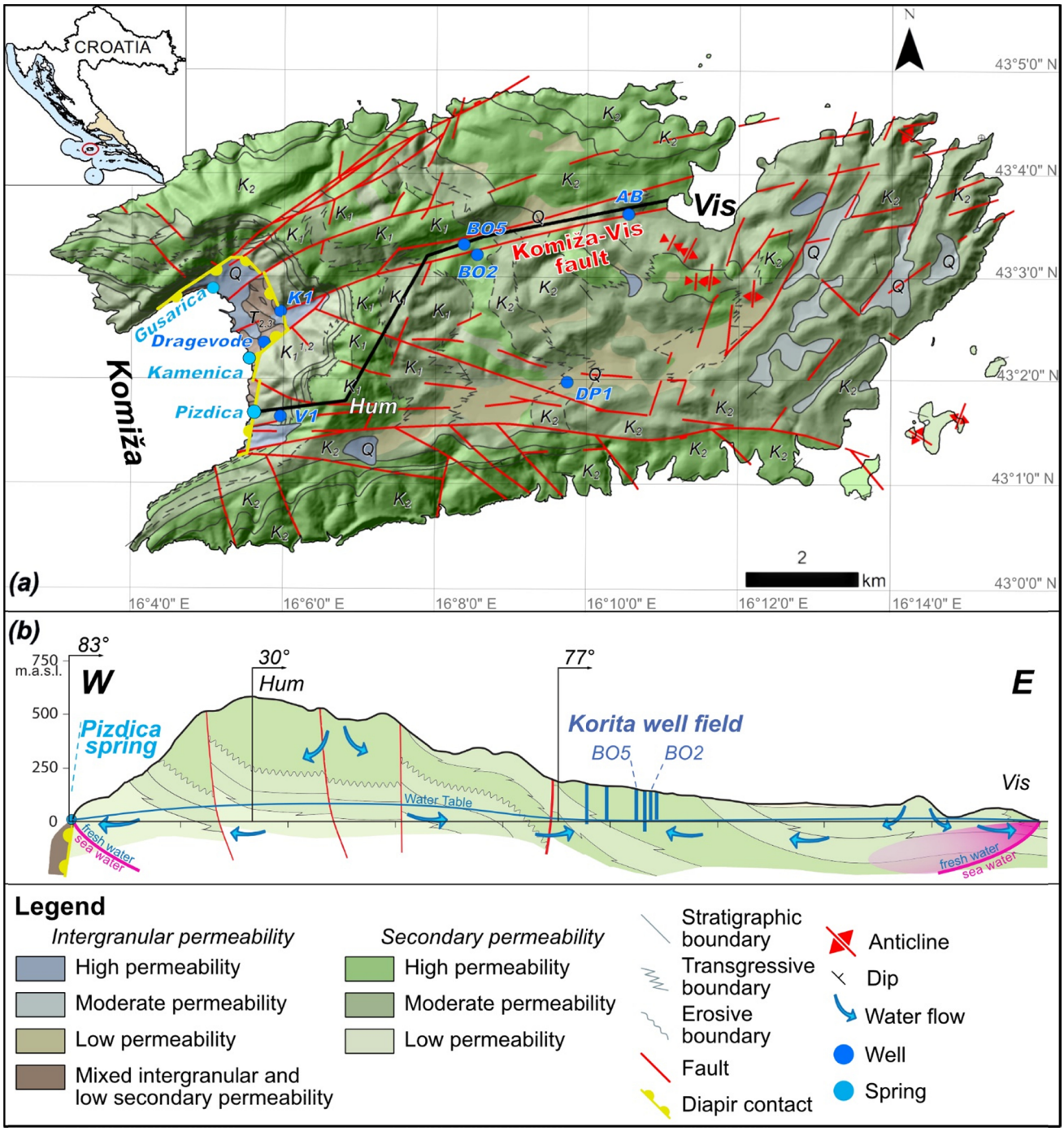

Fig. 1 (a) Hydrogeological map of the island of Vis with sampling locations and geographical position and b) schematic hydrogeological cross section (modified from Terzić et al. 2022). Stratigraphic age: Quaternary (Q), Lower–Upper Cretaceous (K_1–K_2), Middle–Upper Triassic ($T_{2,\ 3}$)

Bonacci et al. 2020). The precipitation is highly seasonal, and more than 70% usually occurs between September and March. There are no permanent surface water bodies on the island, and surface runoff occurs only during intensive rainfall. The average annual potential evapotranspiration factor is approximately 0.65 (Terzić et al. 2022), resulting in an average effective infiltration of 35%, which is concordant with regional coefficients in the Dinaric karst region (Bonacci 2001). Several authors reported significant warming trends related to the air temperature and sea surface temperature, similar to those affecting the entire Mediterranean area (Luterbacher et al. 2006; Bartolini et al. 2012; Krklec et al. 2012; Branković et al. 2013; Bonacci et al. 2020, 2021).

The island is part of the Dinaric karst region, an area characterized by very deep and irregular karstification (Vlahović et al. 2005). The main lithological units, spanning from Middle Triassic to Quaternary (Korbar et al. 2012), comprising the composite structural fabric of the island include (i) Middle–Upper Triassic volcanic-sedimentary-evaporite (VSE) complex of the Komiža bay ($T_{2,3}$), composed of gypsum, dolomite-gypsum breccias, karst debris, and a variety of volcanic and clastic rocks and associated with the uplift of a diapir (bounded by the yellow line in Fig. 1); (ii) Lower – Upper Cretaceous limestones and dolomites (K_1–K_2) that are intensely fractured and karstified; and (iii) Quaternary (Q) deposits, comprised of terra rossa cover in karst poljes, and scattered patches of colluvial deposits and aeolian sands (Korbar et al. 2012). The structure of Vis is an open anticline with a hinge striking E–W and dipping toward the east (Patekar et al. 2022). The island is crosscut by three main sub-vertical faults striking approximately NE–SW, with several minor fault systems of approximately N–S orientation (Fig. 1). The most productive water supply wells (i.e., Korita well field) are associated with the Komiža-Vis fault system that runs through the island's center and enables the infiltration of precipitation as well as gradual karstification of the underlying rock mass (Fig. 1).

Favorable geological and hydrogeological conditions have preconditioned the formation of high-quality karst aquifers from which groundwater is abstracted. Hence, the island is entirely autonomous in terms of water supply. Groundwater is recharged solely by the direct infiltration of precipitation. Terzić (2004) distinguished the five main hydrogeological units that govern the groundwater dynamics on the island of Vis:

- Hydrogeological barriers:
- the VSE complex of the Komiža bay ($T_{2,3}$; Fig. 1). This barrier has a relatively narrow extent in the western coastal zone and prevents seawater intrusion toward the central part of the island. Several springs of various yield are formed at its contact with permeable Quaternary deposits (e.g., Gusarica, Kamenice);
- Quaternary deposits (Q), represented mainly by terra rossa as a thin and discontinuous cover all across the island, and as a thicker layer (up to 45 m; Crnolatac 1953) in karst poljes (e.g., Dračevo polje, Fig. 1). These deposits decrease infiltration, and in the thickest parts of the karst poljes, they act as a local hydrogeological barrier. Additionally, washed-out clayey particles from these deposits provide infill that reduces the permeability of the underlying carbonate rock mass.
- Aquifers:
- low permeability carbonates, represented mainly by Lower Cretaceous well-bedded dolomites (K_1). Although they reinforce the barrier function of the VSE, they are locally fractured and even karstified, allowing groundwater flow in these high-permeability zones (e.g., Pizdica spring, Fig. 1);
- moderate permeability carbonates, comprised of Lower Cretaceous laminated and bedded limestones with dolomitic beds/interbeds, bedded dolomites, and dolomitic breccias in some places (K_1–K_2, Fig. 1). These units are sufficiently permeable to allow groundwater infiltration, accumulation, and flow, and concurrently, not too permeable to allow the excessive penetration of seawater into the island's aquifers;
- high permeability carbonates, mostly represented by Upper Cretaceous highly fractured and karstified thin or thick-bedded limestones (K_1–K_2), situated in northern and southern coastal zones, resulting in groundwater salinization due to the total penetration of seawater. Additionally, these units are present in the central part of the island, forming the most important part of the aquifer, which is protected from significant seawater intrusion by hydrogeological barriers.

The water supply system of Vis consists of five wells (BO1 to BO5) drilled in the Korita well field in the central part of the island, well K1 in the Komiža hinterland, and the coastal spring Pizdica (Fig. 1). The maximum pumping capacity at the Korita well field is 42 l/s (Terzić et al. 2022). Here, groundwater quality is excellent since the wells are positioned in the central part of the island, where the aquifer is protected from seawater intrusion by the impervious VSE complex to the west, as well as by the low permeability carbonates below karst poljes to the south. Additionally, the aquifer is protected by a rock mass of very low permeability (de facto an aquitard) at a few tens of meters below the present sea level (Fig. 1; Terzić et al. 2022). Well K1 and the Pizdica spring in the western part of the island provide approximately 5 l/s in total. Numerous less productive springs and wells on the island are not utilized for public water supply system, but given their historical importance, their resources are still utilized for irrigation or personal use during droughts (e.g., Gusarica, Dragevode, Kamenice; Fig. 1). Approximately 450,000 m^3 of groundwater is abstracted annually from the Korita wells (Patekar et al. 2023), with the majority abstracted during the summer season to sustain a fivefold increase in population due to tourism. Given the island's growing tourism and socio–economic development, increasing groundwater abstraction trends are expected (Patekar et al. 2023). Several reductions for consumers occurred in the last two decades due to low rainfall and declining groundwater levels.

Previous hydrogeological research delineated two distinctive catchments, Korita (19 km^2) and Pizdica

(5 km^2), with an average catchment altitude of 255 and 315 m a.s.l., respectively, and separated by the zonal groundwater divide following the hilly terrain of the Hum ridge (Terzić et al. 2022). Several smaller catchments also exist (e.g., catchments of karst poljes in the south and catchments of springs Kamenice and Gusarica on the rim of VSE) but their relevance in the context of water supply is minor. Groundwater levels usually reach their minimum after the summer (September or October) and maximum after the winter (March or April), with an amplitude of ± 10 m in the Korita water supply wells. The majority of groundwater outflow occurs diffusely through high permeability carbonates along the northern and southern coasts, which prevents detailed observation. Still, few permanent and several periodical vruljas (submarine springs) exist. Pumping test evidenced that even though the karstified carbonate aquifer in the Korita area is quite heterogeneous and consists of voids of different scales that are interconnected by fractures, cracks, and even karst conduits, a homogeneous type of flow through a fractured rock mass prevails, rather than a conduit flow (Terzić et al. 2022). Groundwater exploited in the Korita well field displayed relative stability (e.g., chloride concentrations, electrical conductivity, and pH) despite below-average precipitation during the last five years, suggesting sufficient groundwater reserves with good resilience toward seasonal overexploitation and droughts (Patekar et al. 2022).

Materials and methods

Water sampling and analyses

Measurements of in situ physicochemical parameters and groundwater sampling were conducted monthly from January 2020 to December 2022 and quarterly in 2023. Field measurements and sampling were conducted in (i) deep borewells BO2 and BO5, K1, DP1, and V1, (ii) shallow dug wells Dragevode and AB, and (iii) springs Gusarica, Kamenice, and Pizdica (Fig. 1; Table 1). A total of 376 samples were collected in pre-rinsed 100 mL air-tight polyethylene bottles, sealed, and refrigerated until laboratory analyses, which were conducted within several days of sampling. In situ physicochemical parameters (temperature, pH, and electrical conductivity) were measured using the WTW Multi 3320 multiparameter probe. Alkalinity was measured during the fieldwork using the volumetric titration method by HACH 16900 digital titrator with a 1.6N H_2SO_4 and bromocresol green indicator.

Laboratory analyses were performed in the Hydrochemical Laboratory of the Croatian Geological Survey in Zagreb, Croatia. Analysis of major ions (Ca, Mg, Na, K, SO_4, Cl, and NO_3) was performed by the ion chromatography on the DIONEX ICS-6000 DP (Thermo Fisher Scientific). Stable isotopes of oxygen (^{18}O) and hydrogen (^{2}H) were analyzed using the Picarro L2130-i Isotope and Gas Concentration Analyzer (Picarro, Santa Clara, California, USA), using international standards produced by the USGS (isotope reference material USGS 46, USGS47, and USGS48) for calibration of the results. All isotopic ratio results were reported as δ-notation (‰) relative to the Vienna Standard Mean Ocean Water (VSMOW) standard (Mazor 2004). Furthermore, two sets of samples representing the hydrological minimum and maximum were collected from five characteristic locations and analyzed in the Hydroisotop laboratory in Schweitenkirchen, Germany, to determine the $\delta^{34}S$ and $\delta^{18}O$ values from SO_4^{2-}. Isotope concentrations were measured using the isotope ratio mass spectrometry EA-IRMS method. The isotopic compositions are expressed in the traditional delta notations (‰) with respect to VSMOW standard for oxygen and hydrogen, and CDT (Canon Diablo Troilite) for sulfur. Results were processed in Excel and Diagrammes software (Simler 2012). All acquired samples are within

Table 1 Summary and basic characteristics of analyzed wells and springs on the island of Vis

Name	Type	GWL[a]	Main lithology[b]	Rate[c]
AB	dug well	~14 m	Dolomite	~3 l/s
BO2	borewell	~120 m	Limestone with dolomitic interbeds	< 8 l/s
BO5	borewell	~130 m	Limestone with dolomitic interbeds	< 6 l/s
DP1	borewell	~125 m	Limestone	< 0.5 l/s
Dragevode	dug well	~2 m	Colluvial deposits	Unknown
Gusarica	spring	–	VSE	Unknown
Kamenice	spring	–	Colluvial deposits and VSE	~0.03 l/s
K1	borewell	~68 m	Dolomite and limestone	< 2 l/s
Pizdica	spring	–	Dolomite and VSE	~3.5 l/s
V1	borewell	~155 m	Dolomite	Unknown

[a]depth of groundwater level from the terrain surface (i.e., measured average values), also representing the approximate depth of sampling; [b]simplified and based on the geological and hydrogeological maps (Korbar et al. 2012; Terzić et al. 2022); [c]spring discharge or maximum pumping capacity of the well

the commonly acceptable 5% charge balance error (Appelo and Postma 2005). Graphics and artwork were created in Grapher 10 software.

Hydrochemical and hydrogeological processes

Standard hydrochemical and hydrogeological methods were utilized to assess the occurrence of various processes (e.g., water–rock interactions, mixing of fresh groundwater with seawater, dedolomitization, and ion exchange) in karst aquifers on the island of Vis. Relative ratios of major ions were graphically represented on a trilinear Piper diagram (Piper 1944), and mean concentrations (in meq/l) were plotted in the Schoeller diagram (Schoeller 1962), enabling the identification of groundwater hydrochemical facies, as well as trends and variations in chemical composition, indicating specific hydrogeological processes. Furthermore, diagrams of physicochemical parameters (box-plots of groundwater T, EC, and pH), saturation indices (calcite, dolomite, and gypsum), and specific ionic ratios (i.e., Na/Cl, (Ca + Mg)/(HCO + SO_4), chloro-alkaline indices CAI I and CAI II, and (Ca/(Ca + Mg))/(SO_4/(SO_4 + HCO_3)) were utilized (Schoeller 1965; Frondini 2008; Moral et al. 2008; Tiwari et al. 2019; Cappucci et al. 2020; Zhang et al. 2020; Ismail et al. 2023; Mussa 2023; Sun et al. 2023; Zhang et al. 2023).

Saturation indices (SI) of the main aquifer-forming and related minerals (i.e., calcite, dolomite, gypsum) were calculated based on the equation (Appelo and Postma 2005):

$$\mathrm{SI} = \log\left(\frac{IAP}{K}\right) \tag{1}$$

where IAP is the ion activity product, and K is the solubility product. In karst terrains, SIs serve as a valuable tool for assessing groundwater aggressiveness. SI values indicate the thermodynamic potential for mineral dissolution or precipitation within the aquifer system. Undersaturated conditions (SI < 0) signify that groundwater is aggressive and can dissolve aquifer minerals. Conversely, saturated conditions (SI > 0) suggest that the groundwater is saturated with respect to specific minerals and has the potential to precipitate them (Appelo and Postma 2005). When the SI value is close to 0 or falls within the analytical uncertainty range, the groundwater is considered to be in near-equilibrium with the aquifer minerals. The assumed range of SI uncertainty used in this study is ± 0.1 for calcite and ± 0.5 for dolomite (López-Chicano et al. 2001; Serianz et al. 2020). SIs were calculated using Diagrammes software (Simler 2012).

Furthermore, the seawater percentage (f_{sea}) in groundwater was calculated based on the conservative mixing method proposed by Appelo and Postma (2005). The seawater percentage in a sample (f_{sea}) is defined as:

$$f_{\mathrm{sea}} = \frac{m_{\mathrm{Cl,\ sample}} - m_{\mathrm{Cl,\ fresh}}}{m_{\mathrm{Cl,sea}} - m_{\mathrm{Cl,fresh}}} \times 100(\%) \tag{2}$$

where $m_{Cl,sample}$, $m_{Cl,fresh}$, and $m_{Cl,seawater}$ represent molar concentration of Cl (mmol/l) in a sample, freshwater, and seawater, respectively. If seawater is the only source of Cl, then $m_{Cl,\ fresh}$ equals 0, simplifying Eq. 2 to:

$$f_{\mathrm{sea}} = \frac{m_{\mathrm{Cl,\ sample}}}{602} \tag{3}$$

where $m_{Cl,\ sample}$ is the measured Cl concentration in a sample expressed in mmol/l, and 602 mmol/l is the average Cl concentration of the Adriatic Sea, corresponding to the seawater salinity of 38‰ (Reale et al. 2017).

Chloro-alkaline indices CAI I and CAI II were used to detect ion exchange processes between the matrix of the aquifer and groundwater solution (Schoeller 1965). Positive values of CAI indicate the exchange of Na and K from groundwater solution with Mg and Ca from the aquifer matrix (reverse ion exchange or enrichment in Ca and Mg). In contrast, negative CAI values indicate an exchange of Mg and Ca from groundwater with Na and K from the aquifer matrix (ion exchange or enrichment in Na and K). Generally, CAI indices are close to zero, while higher values indicate stronger ion exchange (Al-Ahmadi 2013; Krishna Kumar et al. 2014). CAI I and II are expressed as (all ions in meq/l):

$$\mathrm{CAI\ I} = \frac{\mathrm{Cl} - (\mathrm{Na} + K)}{\mathrm{Cl}} \tag{4}$$

$$\mathrm{CAI\ II} = \frac{\mathrm{Cl} - (\mathrm{Na} + K)}{\mathrm{CO_3} + \mathrm{SO_4} + \mathrm{HCO_3} + \mathrm{NO_3}} \tag{5}$$

Soluble sodium percentage (%Na), representing the tendency of water to engage in cation exchange reactions in soil, was calculated to assess water quality for agriculture and irrigation. Higher %Na indicates a tendency of sodium cations to adsorb onto clay particle surfaces, potentially leading to reduced soil permeability (Tanvir Rahman et al. 2017). Soluble sodium percentage is calculated as (all ions in meq/l):

$$\%\mathrm{Na} = \frac{\mathrm{Na} \times 100}{\mathrm{Ca} + \mathrm{Mg} + \mathrm{Na} + K} \tag{6}$$

The relationship between soluble sodium percentage and EC was graphically shown on the Wilcox diagram (Wilcox 1955), allowing the classification of water samples into five respective categories.

Results and discussion

Major ion chemistry and physico-chemical parameters

Figure 1 shows the location map of springs and wells analyzed in this study, and Table 1 shows their basic characteristics.

Table 2 shows statistical analyses (minimum, mean, and maximum values, standard deviation) of physicochemical parameters and major ion concentrations of groundwater samples from the island of Vis.

The distribution of groundwater temperature, pH, and EC values is graphically shown in box-plots (Fig. 2).

Groundwater temperatures range from 13 to 23.3 °C (Fig. 2), with mean values between 15.3 and 19.3 °C. At

Table 2 Statistical analyses of in situ physicochemical parameters and hydrochemical components. *n* denotes the number of analyzed samples

Location	Statistics	T	pH	EC	Ca^{2+}	Mg^{2+}	Na^{+}	K^{+}	HCO_3^{-}	SO_4^{2-}	Cl^{-}	NO_3^{-}
		°C	–	µS/cm				mg/l				
AB	Min	14.1	6.89	1527	88.7	40.9	127.2	2.7	340.4	30.0	282.8	0.6
n = 39	Mean	15.9	7.38	1993	124.4	52.7	194.6	7.1	385.6	58.1	424.6	1.2
	Max	18.2	7.83	5880	156.9	124.7	902.1	51.0	438.0	250.1	1827.5	2.7
	St. dev	0.93	0.30	753	9.5	12.1	118.5	7.9	17.5	32.3	234.6	0.6
BO2	Min	14.1	7.25	539	77.1	19.6	21.8	0.4	302.6	8.4	41.6	2.0
n = 39	Mean	15.3	7.44	755	81.9	23.9	32.1	0.9	316.0	11.9	71.8	3.3
	Max	16.2	7.72	917	87.0	29.6	45.6	1.4	342.8	16.2	112.2	6.9
	St. dev	0.5	0.11	89	2.2	2.8	6.7	0.1	8.8	2.0	20.5	0.8
BO5	Min	14.3	7.27	549	81.8	21.2	24.1	0.7	291.6	11.5	45.5	2.6
n = 38	Mean	15.5	7.43	858	89.5	26.7	41.3	0.9	315.5	16.7	103.4	3.8
	Max	17.4	7.73	1058	96.1	33.9	53.8	1.3	340.4	22.2	154.8	4.9
	St. dev	0.7	0.11	118	4.2	2.9	7.7	0.1	9.9	2.5	30.2	0.6
DP1	Min	14.1	6.94	407	59.7	12.8	16.9	0.4	213.5	12.1	27.3	1.0
n = 38	Mean	16.6	7.12	789	110.5	24.2	18.0	8.3	414.7	25.0	41.3	5.6
	Max	18.2	7.85	948	118.5	29.6	19.8	44.8	467.0	39.7	69.1	35.9
	St. dev	0.8	0.18	101	10.2	3.2	0.5	9.2	41.0	4.9	8.6	6.1
Dragevode	Min	13.0	7.44	430	47.9	24.9	17.8	0.1	218.4	31.7	25.5	0.3
n = 39	Mean	16.3	7.77	583	54.1	29.1	19.7	1.2	247.5	48.4	35.5	1.7
	Max	20.2	8.18	843	61.4	35.9	33.5	16.3	292.8	68.6	61.6	3.9
	St. dev	2.2	0.16	79	3.6	3.4	2.6	2.6	19.6	9.2	6.9	1.0
Gusarica	Min	16.3	6.87	812	142.6	23.8	28.9	0.8	318.4	150.6	20.0	3.2
n = 38	Mean	19.3	7.08	1061	155.4	27.7	34.1	1.8	338.0	199.9	64.3	4.8
	Max	23.3	7.57	1179	169.0	34.2	43.6	2.7	362.3	233.9	95.3	10.1
	St. dev	2.2	0.14	87	6.2	2.8	4.3	0.4	8.3	20.9	15.3	1.3
K1	Min	16.6	7.23	716	81.7	26.0	38.7	0.8	317.2	19.3	58.8	3.9
n = 30	Mean	17.7	7.39	875	83.1	35.8	41.0	1.1	371.3	28.1	80.7	5.0
	Max	19.0	7.65	973	84.8	40.5	44.9	1.7	406.3	32.1	120.8	5.8
	St. dev	0.7	0.10	61	0.8	2.9	1.9	0.1	15.0	3.0	11.0	0.5
Kamenice	Min	16.9	6.98	925	119.7	38.3	38.5	0.1	247.7	158.7	48.8	8.0
n = 39	Mean	18.3	7.17	1098	128.4	42.8	40.9	1.3	354.6	191.2	62.6	17.5
	Max	20.5	7.47	1225	149.1	48.7	45.7	5.5	408.7	220.6	78.8	23.0
	St. dev	0.9	0.12	59	5.4	3.3	1.6	0.8	22.6	11.5	6.7	3.1
Pizdica	Min	16.0	7.26	1670	75.0	39.1	195.0	5.0	270.8	60.9	363.4	1.9
n = 39	Mean	16.2	7.44	2011	92.2	45.4	241.0	8.0	299.6	80.2	446.7	3.2
	Max	17.0	7.70	2140	98.2	54.7	279.3	9.4	368.0	91.9	500.7	4.4
	St. dev	0.2	0.11	119	3.9	3.4	13.3	0.7	16.2	8.0	38.3	0.5
V1	Min	15.0	7.30	874	40.7	30.9	91.3	2.3	196.4	2.5	159.7	0.1
n = 37	Mean	16.5	7.51	1324	47.5	35.3	150.2	9.6	236.5	7.6	299.1	0.9
	Max	17.6	7.88	1644	59.5	43.2	180.2	25.1	312.3	18.9	391.4	2.3
	St. dev	0.7	0.13	163	5.0	3.4	19.7	4.5	29.2	4.0	54.6	0.8

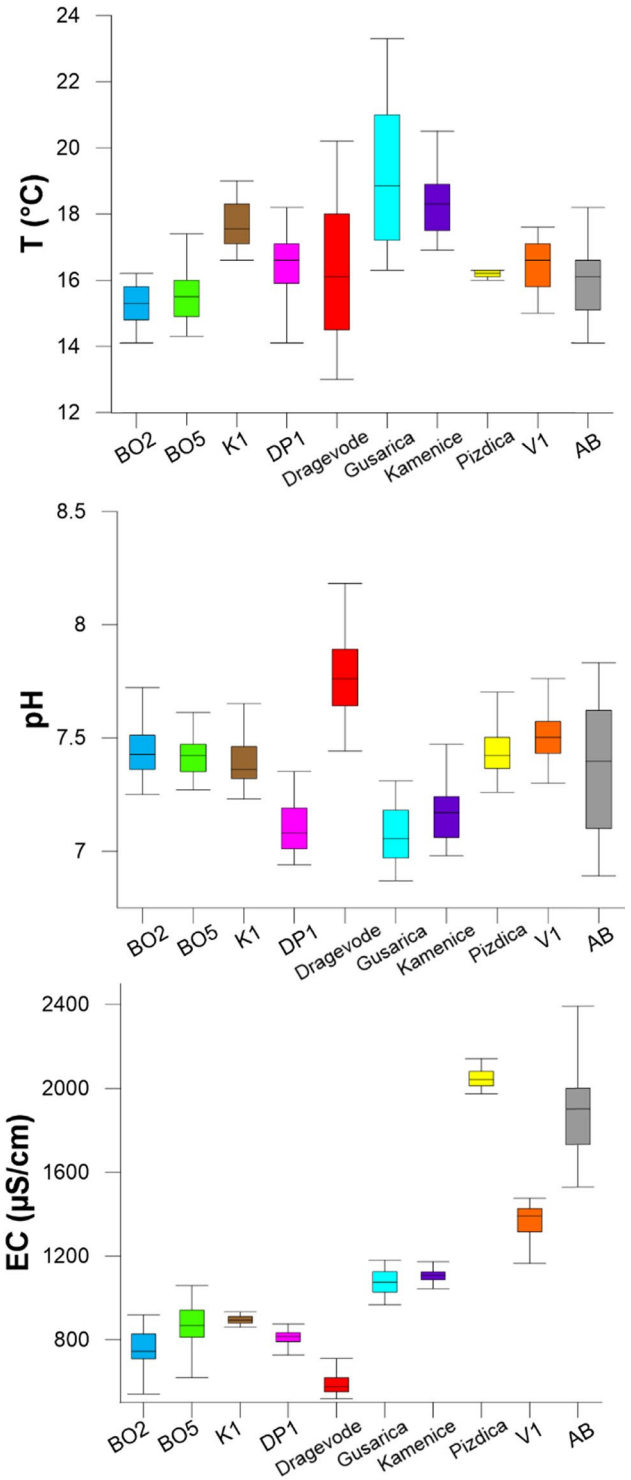

Fig. 2 Box-plots of groundwater temperature, pH, and EC

most investigated locations, the mean annual groundwater temperature is slightly lower than the mean annual air temperature (i.e., 17.2 °C). Deeper borewells (BO2 & 5, DP1, K1, and V1) generally display lower and more stable groundwater temperatures with smaller oscillations, reflecting well depth and deeper groundwater circulation within the aquifer. The lowest variability in groundwater temperature is observed in the Pizdica spring, indicating significant catchment size, high hydraulic gradient in the aquifer, and the dominant role of Pizdica spring in the discharge from this catchment. Smaller springs Kamenice and Gusarica and dug well Dragevode, generally display higher temperature variability due to shallow subsurface groundwater circulation (influenced by air temperature amplitude), while dug well AB is influenced by seawater temperature amplitude.

pH values vary from 6.89 to 8.18, with a mean value of 7.37 (Fig. 2), indicating neutral to mildly alkaline reactions. All groundwater samples are within the pH standard for drinking water (6.5–8.5; EC 2020). The highest pH amplitude is observed in a coastal well AB, and the highest alkalinity in dug well Dragevode.

Electrical conductivity (EC) values range from 516 to 2390 µS/cm (Fig. 2), with several outlier values which were excluded from the plot (i.e., 407 and 5880 µS/cm in DP1 and AB, respectively) due to the scale of the figure. Except in coastal wells V1 and AB, EC values are mostly stable and do not significantly vary despite below-average precipitation during the analyzed period. The main water supply wells BO2, BO5, and K1 display moderate and stable EC (mean values of 755, 858, and 875 µS/cm, respectively). The same stability is observed in the Pizdica spring, with significantly higher EC values (mean value of 2011 µS/cm). The highest variability is observed in the AB well, reflecting the most decisive influence of mixing processes due to tidal fluctuations and low hydraulic gradient in the aquifer.

Ratios of major ions were plotted on the trilinear Piper diagram (Fig. 3), and the mean values of ion concentrations (in meq/l) were plotted on the Schoeller diagram (Fig. 4).

Plotting of data in the Piper diagram (Fig. 3) identified the three dominant hydrochemical facies types of groundwater on the island of Vis:

- Ca–HCO_3 type: BO2, BO5, DP1, K1, and Dragevode
- Mixed type: Gusarica, Kamenice, and AB
- Na–Cl type: Pizdica and V1

All groundwater samples show relative abundance in Ca, Mg, and HCO_3, which is expected given the predominant carbonate lithology of the aquifers on the island of Vis. The first group (squares in Figs. 3 and 4), corresponding to primarily Ca–HCO_3 hydrochemical facies, is characterized by Ca > > Mg > Na > K and HCO_3 > > Cl > SO_4 > NO_3, relatively low EC (mean values < 1000 µS/cm), and low to moderate Cl concentrations. The second group (triangles in Figs. 3 and 4), representing mixed facies, consists of two SO_4-rich groundwater samples from springs Gusarica and Kamenice, where Ca > > Mg > Na > K and

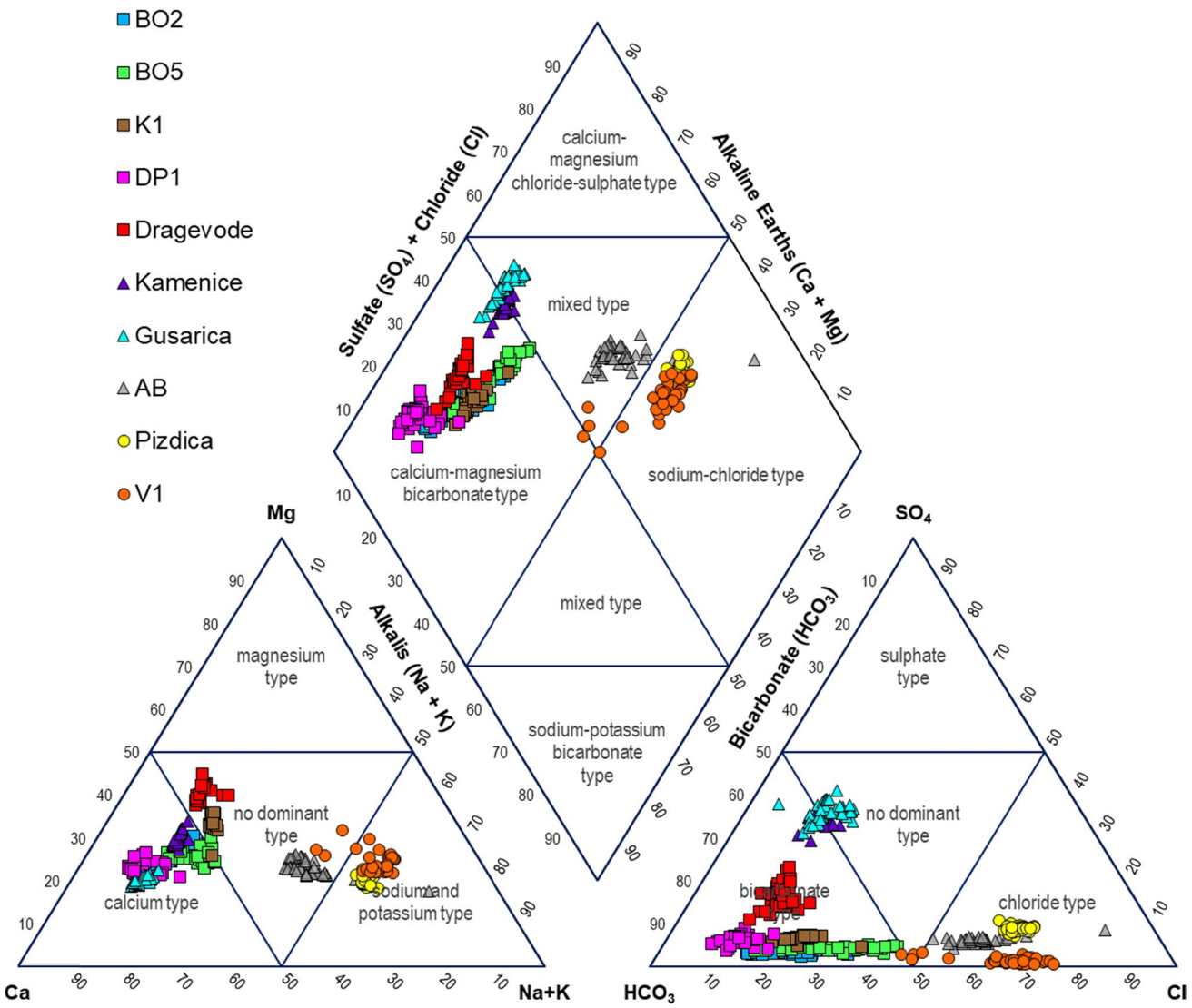

Fig. 3 Piper diagram of groundwater samples from the island of Vis

$HCO_3 > SO_4 > Cl > NO_3$, as well as samples from coastal well AB where Na and Cl prevail. The third group (circles in Figs. 3 and 4) is represented by the Pizdica spring and well V1 with relatively higher Cl concentrations and higher EC values, corresponding primarily to Na–Cl hydrochemical facies. The separation between the three distinctive water groups is relatively well-defined, while the intermediate chemical composition of some groundwater samples reflects the higher effect of specific hydrogeological processes on groundwater chemistry (e.g., stronger mixing with seawater, stronger dissolution of gypsum).

Table 3 shows the Pearson correlation coefficient between the investigated hydrochemical variables of the bulk dataset. The strongest positive correlation is evident between EC and dissolved ions (i.e., Mg, Na, and Cl), which primarily contribute to groundwater mineralization and salinization. A high correlation of Ca with HCO_3 and SO_4 indicates a strong effect of the dissolution of carbonate and sulfate minerals on groundwater chemistry, while a strong correlation of Na and Cl is logical and expected on an island. The negative correlation of pH with Ca and HCO_3 is also expected, given the nature of carbonate dissolution (Ford and Williams 2007).

Chemical equilibrium for a specific mineral is commonly investigated by calculating the saturation index (Eq. 1). In Fig. 5, saturation indices for calcite and dolomite were plotted. Additionally, saturation indices for gypsum were plotted as a function of SO_4 concentration (Fig. 6). Almost all groundwater samples are oversaturated or in equilibrium with respect to calcite, regardless of Cl and SO_4 concentrations. Undersaturation with respect to calcite is evident only in a dozen samples from well V1, along

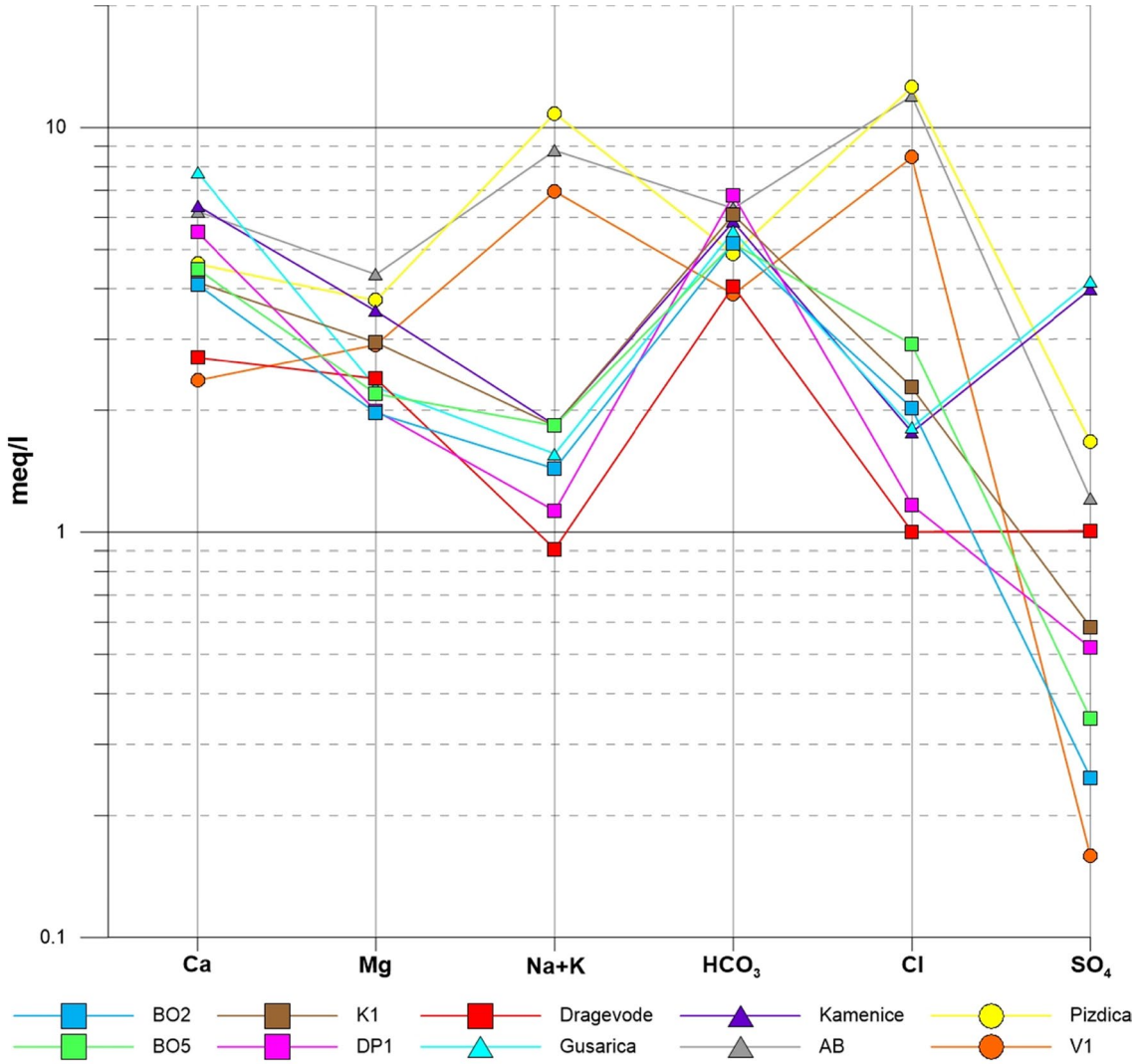

Fig. 4 Schoeller diagram of groundwater samples from the island of Vis, showing the mean ion concentrations from the analyzed period

Table 3 Pearson correlation coefficients between the investigated hydrochemical variables

T	1										
pH	−0.47	1									
EC	−0.04	−0.07	1								
Ca	0.43	**−0.67**	0.24	1							
Mg	0.04	0.00	**0.83**	0.21	1						
Na	−0.17	0.13	**0.92**	−0.03	**0.78**	1					
K	−0.10	−0.02	**0.52**	−0.04	0.38	**0.58**	1				
Cl	−0.19	0.13	**0.92**	−0.02	**0.78**	**0.99**	**0.59**	1			
HCO_3	0.18	**−0.58**	0.07	**0.67**	0.12	−0.15	0.02	−0.12	1		
SO_4	**0.59**	−0.44	0.18	**0.74**	0.28	−0.01	−0.10	−0.05	0.17	1	
NO_3	0.32	−0.40	−0.12	0.39	0.10	−0.25	−0.19	−0.29	0.25	**0.56**	1
	T	pH	EC	Ca	Mg	Na	K	Cl	HCO_3	SO_4	NO_3

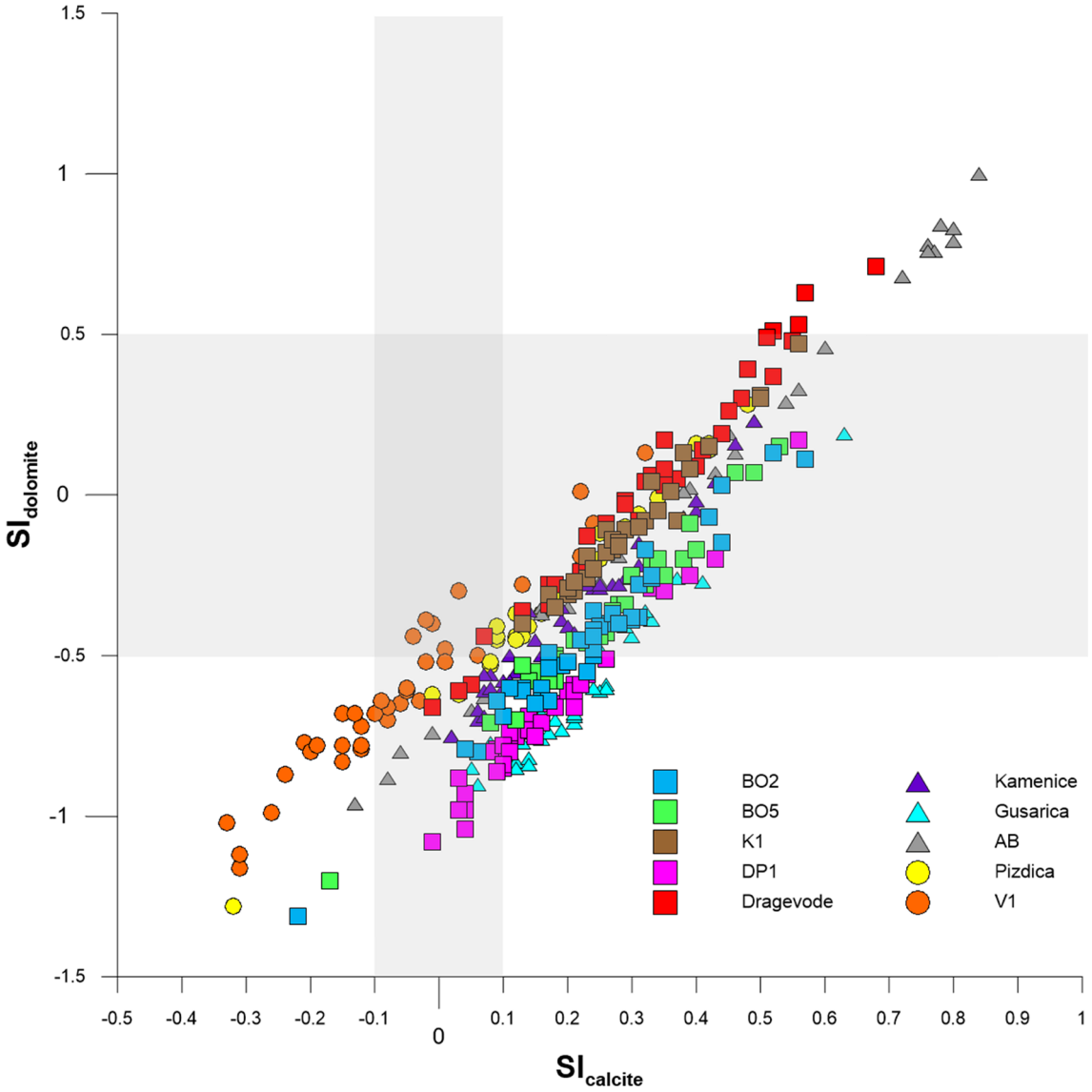

Fig. 5 Saturation indices (SI) of dolomite and calcite. Gray rectangles indicate equilibrium (±0.1 for calcite and ±0.5 for dolomite)

with several scattered samples from other locations. Such undersaturation might result from higher transmissivity in well V1 and lower groundwater residence time, which is also indicated by relatively low mineralization (Table 2). Furthermore, approximately half of groundwater samples from all three groups are in equilibrium, while the rest are strongly undersaturated with respect to dolomite. $SI_{dolomite}$ has a significantly higher range of distribution than $SI_{calcite}$, from − 1.31 to 1.01, with most groundwater samples with $SI_{dolomite}$ between 0 and − 1. Saturation indices for gypsum show a good correlation to increasing SO_4 concentrations and are strongly undersaturated in the majority of the groundwater samples (Fig. 6), except in the mixed group (Gusarica and Kamenice), where the lowest undersaturation is evidenced, indicating the strongest effect of dissolution of sulfate minerals, followed by the well AB and the Pizdica spring. In the former, sulfates are exclusively derived from seawater, while in the latter, there is some sulfate mineral dissolution due to the presence of gypsum and anhydrite outcrops in the discharge zone of the spring. There are no observable differences in the trends of saturation indices between wells and springs.

The isotopic composition of $\delta^{18}O$ and $\delta^{2}H$ of all collected groundwater samples is shown in Fig. 7. As precipitation was not collected during the monitoring period, data from the IAEA GNIP database (IAEA/WMO 2006) were used to construct the local meteoric water line (LMWL). For the construction of the LMWL, we excluded three rain samples (from the summer months) with a d-excess value close to zero or negative and a low amount of precipitation (a few

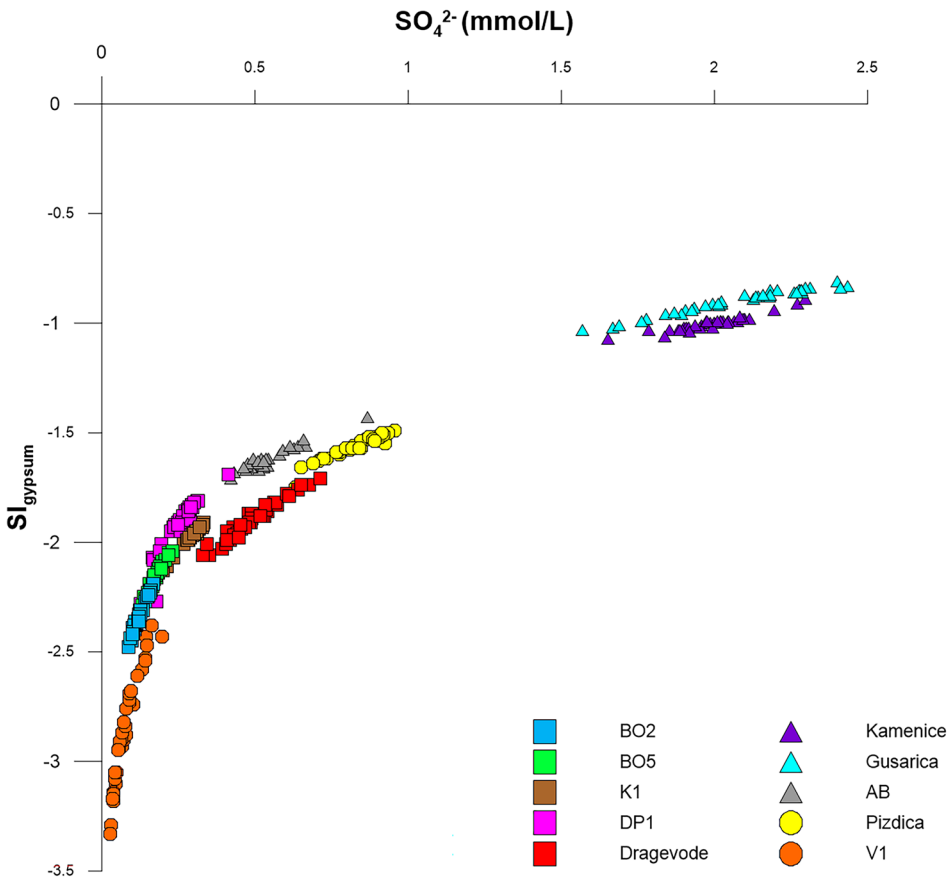

Fig. 6 Saturation indices of gypsum versus dissolved SO_4

mm) due to the possibility of evaporation of the samples. The precipitation samples used for the construction of the LMWL were collected from September 2000 to December 2003 (IAEA 2005). The rain gauge station was located near the coast in Komiža. In order to take into account the infiltration of precipitation in the system, the mean precipitation values were weighted by the amount of precipitation. The calculated amount weighted mean of precipitation was $\delta^{18}O = -6.52‰$, and $\delta^{2}H = -39.91‰$, and d-excess of 13.23‰. The average $\delta^{18}O$ content of all collected samples ranged from −6.11‰ in DP1 to −6.99 ‰ in K1, and the average $\delta^{2}H$ content ranged from −34.56‰ in DP1 to −39.85‰ in K1. The average d-excess values ranged from 14.28 to 16.91‰. The isotopic content of the collected samples and the precipitation confirms the meteoric recharge of the aquifer. The slightly higher d-excess values in the samples in relation to precipitation can be attributed to the altitude effect, as the rain gauge is located near the coast at 6 m a.s.l. and the recharge area of the springs and borewells reaches up to almost 500 m a.s.l.

Water–rock interactions

Piper diagram and statistical distribution of hydrochemical components indicated several intertwined processes in different temporal and spatial scales affecting the groundwater chemistry on the island of Vis. These processes include (i) water–rock interactions (mixed dissolution of limestone and dolomite within the karst aquifers, dissolution of evaporite minerals from the VSE complex, and dedolomitization), (ii) chloride enrichment (seawater intrusion, infiltration of Cl-rich marine aerosols, or atmospheric contribution), (iii) reverse ion exchange, and (iv) anthropogenic pollution.

Given the composite lithological structure of the island of Vis, the molar ratios Ca/(Ca + Mg) and $SO_4/(SO_4 + HCO_3)$ were utilized to assess the dominant dissolution process in groundwater samples on the island of Vis (Fig. 8). Ca/(Ca + Mg) ratio commonly ranges from 0.5 to 1, representing the dissolution of stoichiometric dolomite and calcite (i.e., pure limestone), respectively. Additionally, an increase in SO_4 concentration is indicative of the dissolution of sulfate minerals. The diagram in Fig. 8 shows predominantly dolomite dissolution in samples from the Na–Cl group, while samples from the Ca–HCO_3 group are characterized by intermediate values, implying mixed dissolution of limestone and dolomite. Samples from the mixed group

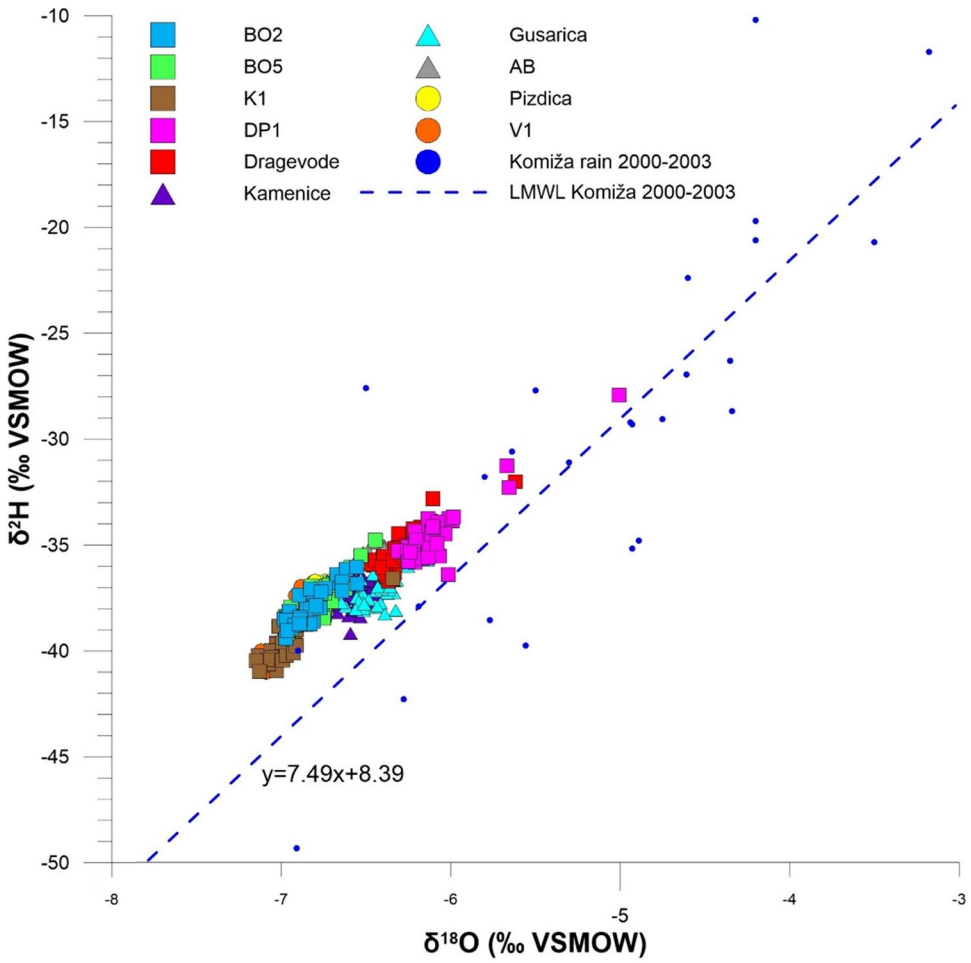

Fig. 7 Isotopic composition δ^2H and $\delta^{18}O$ of groundwater samples from the island of Vis with calculated LMWL for Komiža

are also characterized by mixed dissolution of limestone and dolomite, whereas springs Kamenice and Gusarica show a significant increase in SO_4 concentrations and plot toward gypsum end member. Both springs occur within the zone of the VSE complex of the Komiža bay, where scattered gypsum outcrops are commonly found on the surface. Gypsum and anhydrite outcrops are also present in the discharge zone of the Pizdica spring, whose groundwater is characterized by intermediate values of SO_4. Conversely, well V1, which is located in the hinterland and catchment of the Pizdica spring, shows the lowest values of SO_4, confirming the relatively narrow extent of the VSE zone in the western part of the island. A minor effect of gypsum dissolution is reflected in SO_4 concentration in dug well Dragevode, which is also located in the zone of the VSE complex. Furthermore, a relative increase in Mg accompanied by an increase in SO_4 suggests that groundwater from springs Gusarica and Kamenice is affected by dedolomitization, a common process in aquifers which contain both dolomite and gypsum (Plummer et al. 1990; Capaccioni et al. 2001). The mechanism of dedolomitization is driven by the dissolution of gypsum, causing excess Ca and calcite precipitation, and the consequent dissolution of dolomite followed by an increase of Mg in the groundwater (Appelo and Postma 2005). These groundwaters are also slightly or strongly oversaturated with respect to calcite (Fig. 5) and show an increase in Ca and Mg and a decrease in pH with increasing SO_4, which is expected under conditions of dedolomitization.

To assess the temporal and spatial variations of isotopic composition and concentrations of the dissolved sulfate, $\delta^{34}S$ and $\delta^{18}O$ from SO_4 have been investigated during the hydrological minimum and maximum in September 2020 and January 2021, respectively. Based on the concentration of $\delta^{34}S$ and $\delta^{18}O$ isotopes, possible sources of sulfate include (i) atmospheric deposition, (ii) soil sulfate, (iii) oxidation of reduced inorganic sulfur compounds, (iv) dissolution of evaporites, and (v) marine origin (Porowski et al. 2019). Results and summary of various sulfate sources in groundwater from the island of Vis are shown in Fig. 9. Samples from all investigated locations plot similarly in both hydrological scenarios, and are in concordance with

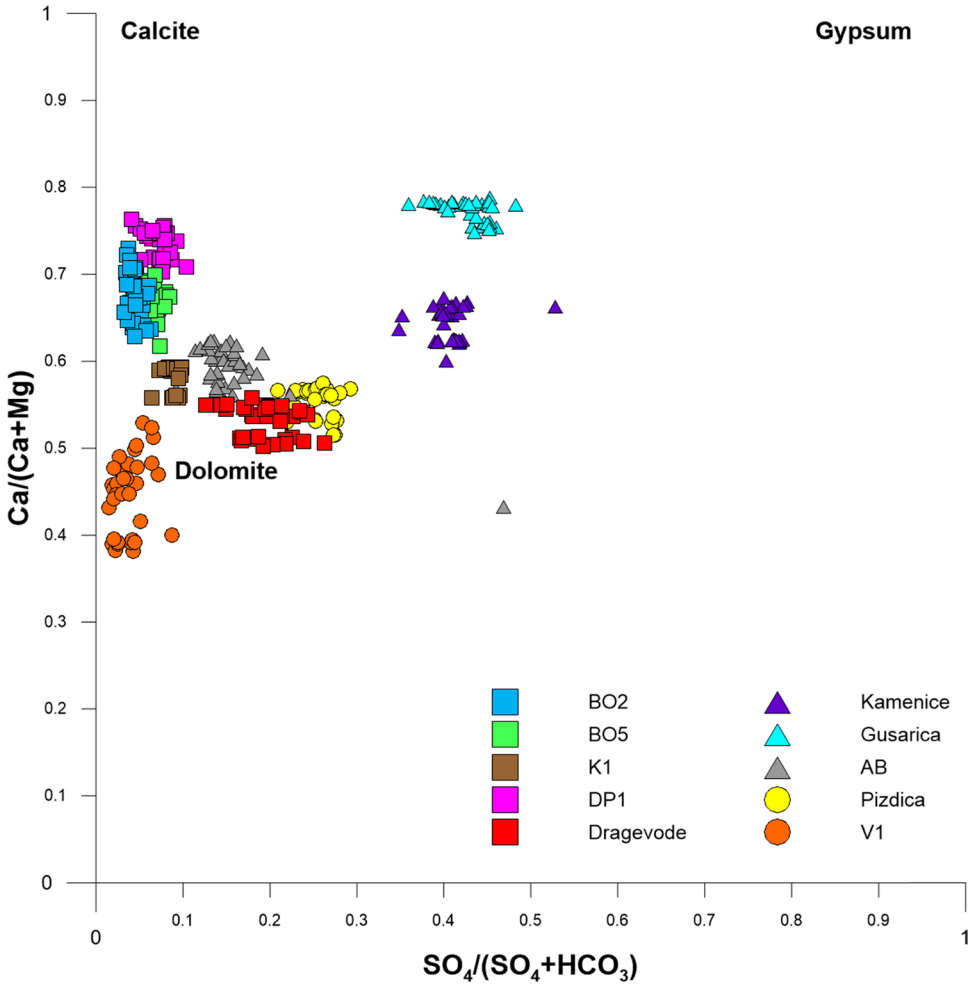

Fig. 8 Diagram of Ca/(Ca + Mg) and SO_4/(SO_4 + HCO_3) molar ratios

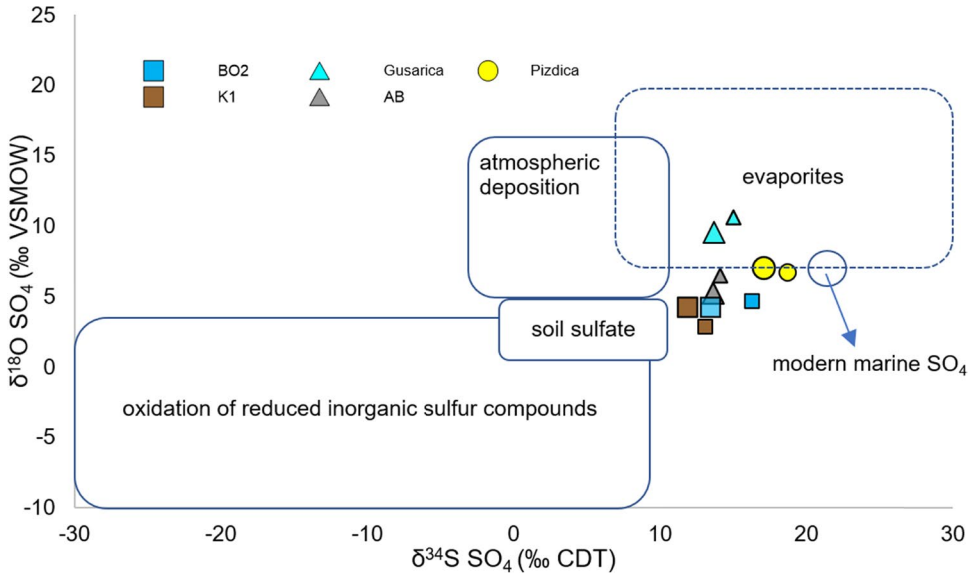

Fig. 9 Bivariate diagram of $\delta^{34}S$ versus $\delta^{18}O$ from SO_4, reflecting typical sulfate sources. Samples from hydrological maximum are represented by larger symbols and vice versa. Modified after Porowski et al. (2019)

the local geological setting. In particular, samples from the Gusarica spring indicate gypsum dissolution as the primary source of SO_4, as the spring is located in the VSE complex adjacent to surface gypsum outcrops. A lesser effect of gypsum dissolution is observed at the Pizdica spring, with a slight downward shift indicating stronger marine influence,

in accordance with its Na–Cl hydrochemical facies. Samples from water supply wells BO2 and K1 show mixed influence of atmospheric deposition, modern marine SO_4, and soil sulfate. During the hydrological maximum, SO_4 contribution from precipitation and topsoil percolation is higher, whereas, during the minimum, a slight shift toward marine influence is most likely related to the increased mixing process of groundwater and seawater. Samples from well AB plot closely to BO2 and K1, but with a slight upward shift bordering the zone of evaporite dissolution during the hydrological minimum. However, given the absence of evaporite deposits in the eastern part of the island (the most distant part with respect to the VSE complex of the Komiža bay), the most likely origin of these sulfates is a combination of atmospheric deposition and a stronger marine influence.

Seawater intrusion and mixing processes

The molar ratio of Na and Cl was explored to investigate the occurrence, source, and extent of groundwater salinization on the island of Vis (Fig. 10). The ratio of 1:1 implies the dissolution of pure halite, and a higher ratio indicates excess Na as a result of weathering of silicate minerals or cation exchange processes, whereas Na and Cl ratios lower than those of seawater (i.e., 0.86) indicate seawater intrusion, reverse ion exchange or anthropogenic contamination (Mercado 1985; Appelo and Postma 2005; Abu-alnaeem et al. 2018). Since no halite mineralization was ever recorded on the island of Vis, the possible sources of salinization are seawater intrusion, infiltration of chloride-rich marine aerosols, and atmospheric deposition. Two distinctive clusters are evident in Fig. 10, Ca–HCO_3 group and mixed group (springs Kamenice and Gusarica) with low concentrations of Na and Cl, and Na–Cl group and coastal well AB with significantly higher concentrations of Na and Cl. This is concordant with the structural fabric of the island, where high permeability carbonates, situated along the coast, act as preferential flow paths for seawater intrusion, hence the higher concentrations in the Na–Cl group. Conversely, geological structures and hydrogeological barriers impede significant intrusion in more distant wells and springs of the low salinity Ca–HCO_3 group. The fact that even the most salinized groundwater from the island of Vis displays mean chloride concentrations on the threshold of fresh water

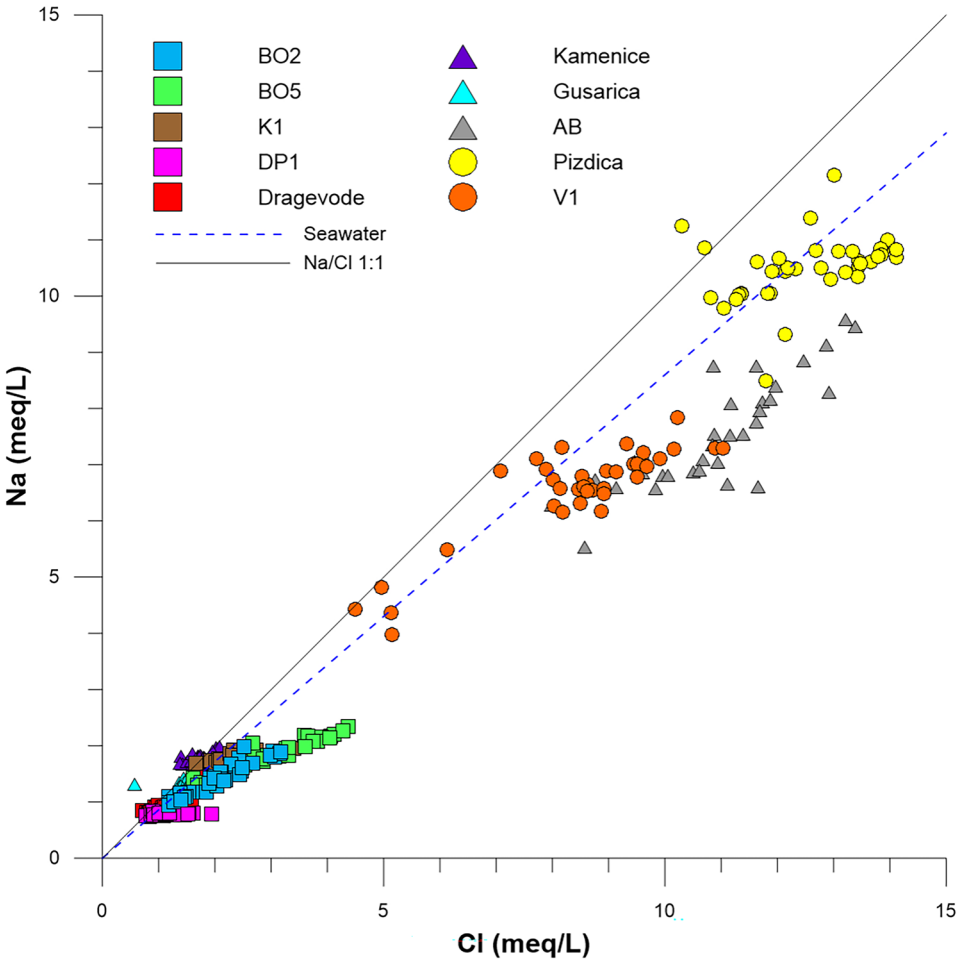

Fig. 10 Biplot diagram of Na and Cl molar ratios

Table 4 Seawater percentage (f_{sea}) in groundwater samples from the island of Vis and comparison with the historical data from 1999/2000

	f_{sea} (%)			
	Min	Mean	Max	1999/2000[a]
BO2	0.19	0.34	0.53	0.38–0.43
BO5	0.21	0.48	0.73	n.a
K1	0.28	0.38	0.57	0.19–0.23
DP1	0.13	0.19	0.32	n.a
Dragevode	0.12	0.17	0.23	0.20
Kamenice	0.23	0.29	0.37	0.38–0.52
Gusarica	0.09	0.30	0.45	0.35–0.39
AB	1.33	1.99	8.56	n.a
Pizdica	1.70	2.09	2.35	1.95–2.48
V1	0.75	1.40	1.83	n.a

[a]data from Terzić (2004)

and brackish water indicates that seawater intrusion is not too extensive even during prolonged dry periods, implying favorable and balanced hydrostatic regime with relatively small but sufficient fresh groundwater reserves within the island's aquifers.

The seawater percentages in groundwater samples were calculated by a simplified approach to the conservative mixing method (Eq. 3) and are shown in Table 4. The seawater percentage is very low (< 1%) in the majority of the samples, except in the Na–Cl group and well AB (> 1%). f_{sea} values higher than 2% are considered a taste-based threshold when water becomes salty, while f_{sea} of 4% is the threshold for human consumption (Mahlknecht et al. 2017). By comparing the available data from previous campaigns in 1999/2000 (Terzić 2004) with the data presented in this study, there are no significant differences in f_{sea} values in any investigated locations (except in water supply well K1). However, these conclusions are based on limited data and cannot be considered as fully representative. Additionally, it is noteworthy that pumping rates increased by 30 to 40% in the Korita water supply wells BO2 and BO5 during the early 2000s.

The simplified approach to estimating f_{sea} presumes the concentration of Cl in local precipitation (atmospheric deposition) to be zero. Although the detailed ionic composition of local precipitation had not been investigated before, Skevin-Sović et al. (2012) reported the mean Cl concentrations of 7.1 g/m^2 annually in wet deposition at the meteorological station in Komiža. Long-term sampling of wet and dry atmospheric depositions is necessary to accurately estimate the concentrations and mechanisms of atmospheric Cl contribution to the local groundwater, with the eventual reambulation of the empirical relationship in Eq. 3 to account for the local conditions more accurately. Regardless, given the island setting of the study area, it is presumable that seawater intrusion has a significantly stronger effect on groundwater Cl concentration. Hence, f_{sea} values obtained through a simplified approach could be considered as realistic. Furthermore, another possible source of chlorides is the infiltration of chloride-rich marine aerosols blown over the island's surface during strong winds. Physicochemical data indicate that EC values and Cl concentrations of groundwater generally decrease after rain at all investigated locations, excluding the infiltration of chloride-rich marine aerosols as a major contributor to groundwater salinization. Therefore, the primary origin of the saline content in groundwater on the island of Vis is the diffuse mixing of fresh groundwater and seawater.

Considerable Cl concentrations and EC (Table 2) in some samples from the Ca–HCO_3 group imply that a certain degree of mixing with seawater occurs even in aquifers protected by the distinctive hydrogeological barriers. To illustrate, slight deviation and excess chlorides are visible in water supply wells BO5 and, to a lesser extent, in BO2 (Fig. 10). Given the presence of relatively watertight rock mass (dolomitic intrabed) below the Korita well field, at several tens of meters below the sea level, coupled with hydrogeological barriers from the W (impermeable VSE complex) and the S (infilled rock mass of low permeability below karst poljes), the small fraction of seawater reaches the aquifer below Korita well field most likely via deeper faults, either through the main E–W fault (Komiža-Vis fault) or lower-order NE–SW faults (Fig. 1). The highest levels of chlorides coincided with the lowest precipitation and the highest pumping rates to sustain intensive summer tourism, implying that older, deeper, and more mineralized groundwater was abstracted. This could also indicate that seawater upconing occurs below the Korita well field during groundwater minimum, causing a small degree of mixing despite the presence of relatively watertight dolomitic intrabed in the base of the aquifer.

Ion exchange

The Na and Cl ratio can also indicate ion exchange and reverse ion exchange processes (Zaidi et al. 2015). In Fig. 10, slight excess of Cl over Na in several samples from the Ca–HCO_3 group (e.g., BO5 and K1) and even higher Cl excess in the Na–Cl and mixed group (Pizdica, V1, and AB) may be indicative of a well-known geochemical effect induced by the seawater intrusion into freshwater aquifer, i.e., reverse ion exchange, where Ca is exchanged by Na in the carbonate matrix, resulting in an increase of Ca and a decrease of Na concentrations in groundwater (Zaidi et al. 2015; Colombani et al. 2017; Mora et al. 2020). To validate whether reverse ion exchange occurs in groundwater samples from the island of Vis, molar ratios of $(Ca+Mg)/(HCO_3+SO_4)$ are plotted in Fig. 11. Most groundwater samples plot close to the equiline or above, indicating that groundwater chemistry on the island of Vis is controlled

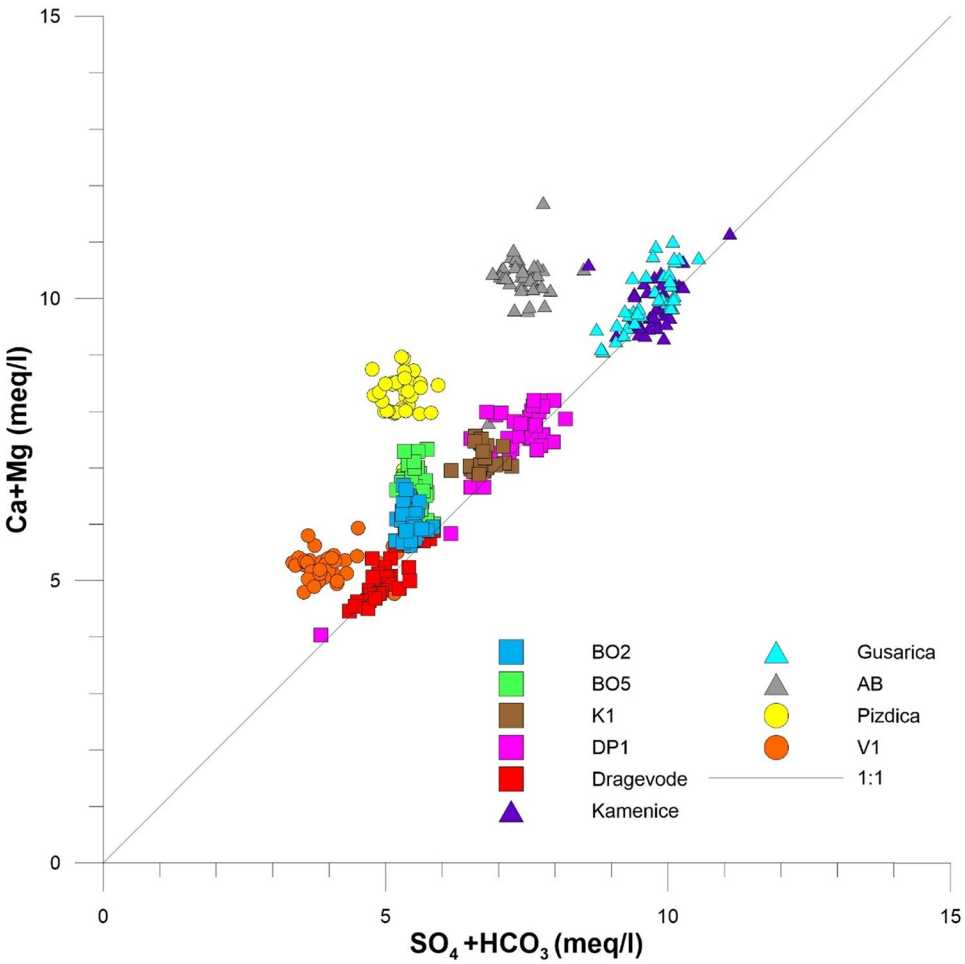

Fig. 11 Biplot diagram of $(Ca+Mg)/(HCO_3+SO_4)$

by the combination of carbonate and sulfate dissolution, as well as reverse ion exchange as a consequence of mixing processes. The upward shift appears concordantly to the Na/Cl plot, and a stronger effect of reverse ion exchange occurs in samples with higher Cl concentrations (i.e., AB, Pizdica, and V1).

Chloro-alkaline indices (Schoeller 1965) CAI I (Eq. 4) and CAI II (Eq. 5) shown in Fig. 12 point to the same trends as previous plots, confirming the occurrence and effect of reverse ion exchange on groundwater chemistry. The amplitude of CAI I goes from − 0.33 to 0.48, while CAI II values range from –0.05 to 1.03. CAI indices reveal that stronger exchange reactions occur with increasing chloride concentrations. In contrast, both indices reach their minimum during the recharge period, indicating a significantly lesser influx of both Na and Cl through diffuse or preferential seawater intrusion. Due to the absence of groundwaters characterized by Ca–Cl or Na–HCO_3 type hydrochemical facies (Fig. 3), representing the end members in groundwater evolution in (reverse) ion exchange pathways, respectively, it is possible to infer that reverse ion exchange plays a subordinate role with respect to carbonate dissolution in the evolution of the local groundwater chemistry. This is most likely due to a relatively low degree of seawater intrusion and mixing with fresh groundwater, even in the Na–Cl group, whose groundwaters are in the brackish water domain (Cl from 300 to 1000 mg/l), even during hydrological minimum. Negative values of CAI indices are characteristic for only a dozen samples, indicating a very weak ion exchange reaction.

Implications of local groundwater chemistry on the water supply and agriculture

Amplitudes of parameters from three hydrochemical groups analyzed in the scope of this study were evaluated with respect to the prescribed recommendations by the World Health Organization (WHO 1997), and the maximum allowed concentration prescribed by the Europan Union (EC 2020) and Croatian legislation (MHSS 2008) regarding drinking water quality. Ca–HCO_3 group exhibits all parameters within the standards (Table 5), the mixed group displays very high EC, TDS, Na, and Cl (due to variable seawater intrusion in well AB), and

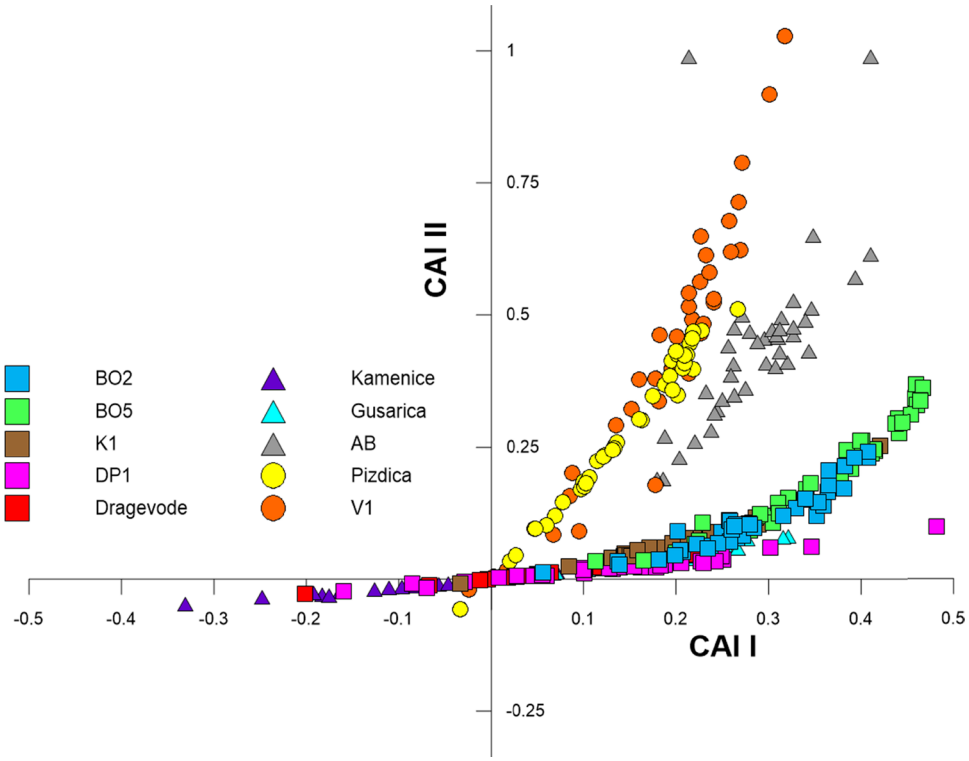

Fig. 12 Bivariate diagram of CAI I and CAI II indices

Table 5 Comparison of analyzed parameters with standards for drinking water. Values higher than recommended or allowed are highlighted in red

	Hydrochemical group						Standard	
	Ca-HCO_3		Mixed		Na-Cl		WHO	EC and MHSS
	Min.	Max.	Min.	Max.	Min.	Max.	Threshold values	
pH (-)	6.94	8.18	6.87	7.83	7.26	7.88	6.5–8.5	6.5–8.5
EC (µS/cm)	407	1058	812	5880	874	2140	1500	2500
TDS (mg/l)	369	739	748	3676	673	1320	1500	-
Ca (mg/l)	47.9	118.5	88.7	169.0	40.7	98.2	200	-
Mg (mg/l)	12.8	40.5	23.8	124.7	30.9	54.7	150	-
Na (mg/l)	16.9	53.8	28.9	902.1	91.3	279.3	200	200
K (mg/l)	0.1	44.8	0.1	51.0	2.3	25.1	200	-
HCO_3 (mg/l)	213.5	467.0	247.7	438.0	196.4	368.0	600	-
Cl (mg/l)	25.5	154.8	20.0	1827.5	159.7	500.7	600	250
SO_4 (mg/l)	8.4	68.6	30.0	250.1	2.5	91.9	600	250
NO_3 (mg/l)	0.3	35.9	0.6	23.0	0.1	4.4	50	50

borderline SO_4 values (seawater intrusion in AB and gypsum dissolution in springs Kamenice and Gusarica), whereas in the Na–Cl group, the most critical parameters are EC, Na, and Cl due to seawater intrusion.

Owing to the excellent water quality of the Ca–HCO_3 group, the island of Vis has one of the highest quality raw groundwater and potable water among the Adriatic and Mediterranean islands (Al Haj et al. 2023). There are no significant industrial pollution sources on the island, and most sewage systems are located in coastal areas (practically at sea level), so the exploited groundwater is subjected only to chlorination treatment before distribution to eliminate potential bacterial contamination. Groundwater from karst aquifers commonly exhibits high natural bacterial count due to the intrinsic properties of such aquifers (e.g., rapid infiltration, lack of soil and sediment filtration; Vučinić et al. 2023; Fernández-Ortega et al. 2024). Agricultural pollution, commonly identified by NO_3, was evidenced only at the Kamenice spring and well DP1 since both are located adjacent to agricultural areas. All water supply wells show very low concentrations of NO_3 (Tables 2 and 5) since most agricultural areas are located downstream with respect

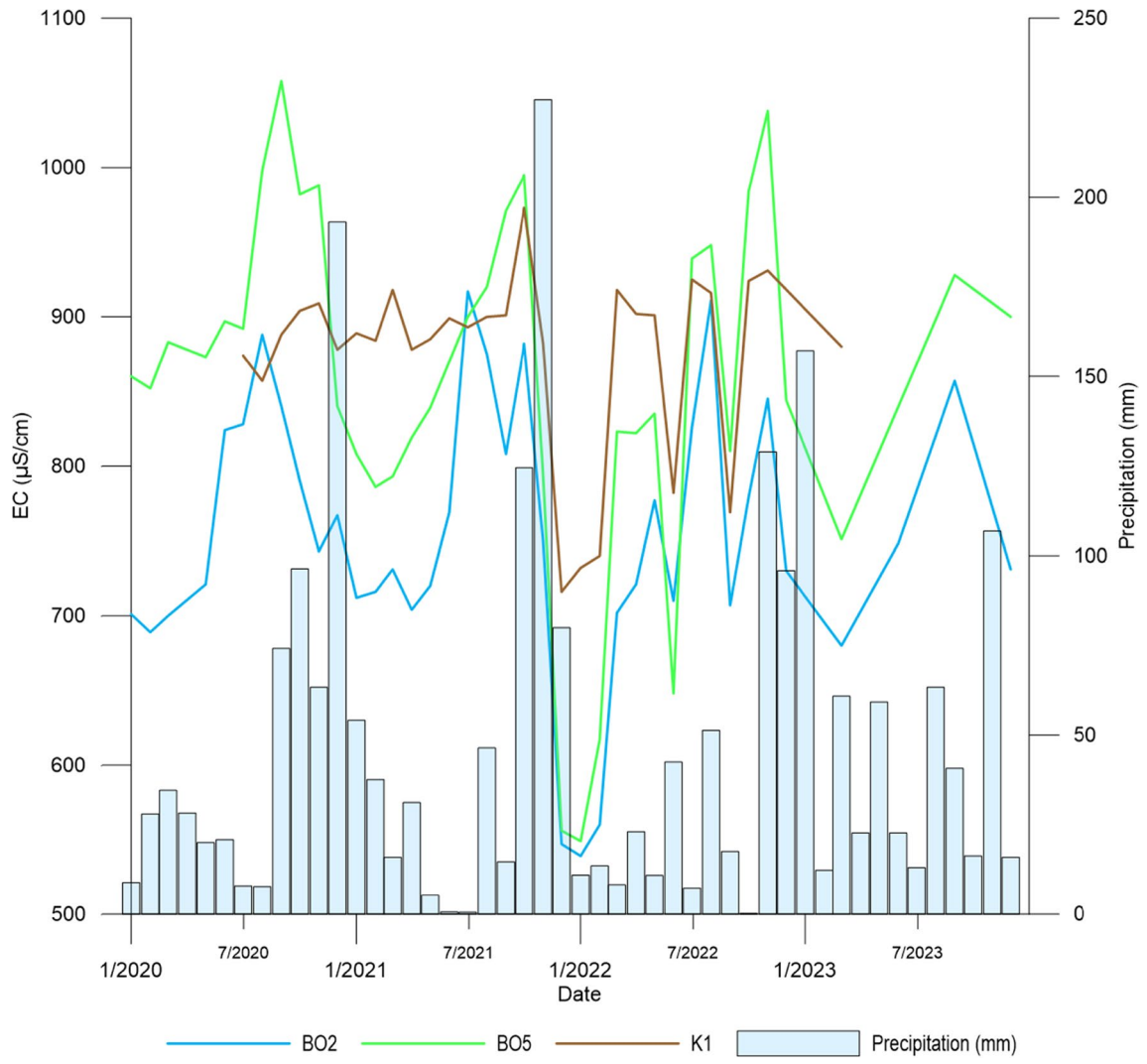

Fig. 13 Time series of groundwater EC and monthly precipitation

to water supply wells. Due to the higher Cl concentration in groundwater at the Pizdica spring (above the drinking water standard of 250 mg/l), it is mixed in a ratio of 1:4 with groundwater from the Korita well field and K1 well.

The time series of groundwater EC in water supply wells BO2, BO5, and K1 versus monthly precipitation (measured at the meteorological station in Komiža) were plotted in Fig. 13. Peaks in EC values occur during the summer, characterized by very low precipitation, high water demand due to tourism, and a non-stop operational regime of pumping wells. In all three wells, EC drops sharply after the infiltration of precipitation (Fig. 13). Notably, the investigated period was characterized by significantly lower precipitation with respect to the 30-year average value of 745 mm/a, with 583, 638, 410, and 591 mm/a in the period from 2020 to 2023, respectively, whereas the annual groundwater exploitation remained practically the same throughout the investigated period.

Groundwater from wells and springs that are not included in the water supply system is utilized either as technical water (e.g., Gusarica), irrigation water (e.g., Dragevode), or for personal use (e.g., Kamenice). The quality of water for agriculture and irrigation was assessed by the Wilcox diagram (Fig. 14), representing the relationship between EC and soluble sodium percentage (%Na; Eq. 6). Samples from the Ca–HCO_3 and the mixed group (Kamenice and Gusarica) plot into excellent and good categories, whereas samples from the Na–Cl group and AB from the mixed group span across good, permissible, doubtful, and even unsuitable categories. With the recent improvements and expansions of the water supply system on the island of Vis, higher-quality irrigation water is available to farmers. However, this raises many issues regarding sustainability and may lead to local

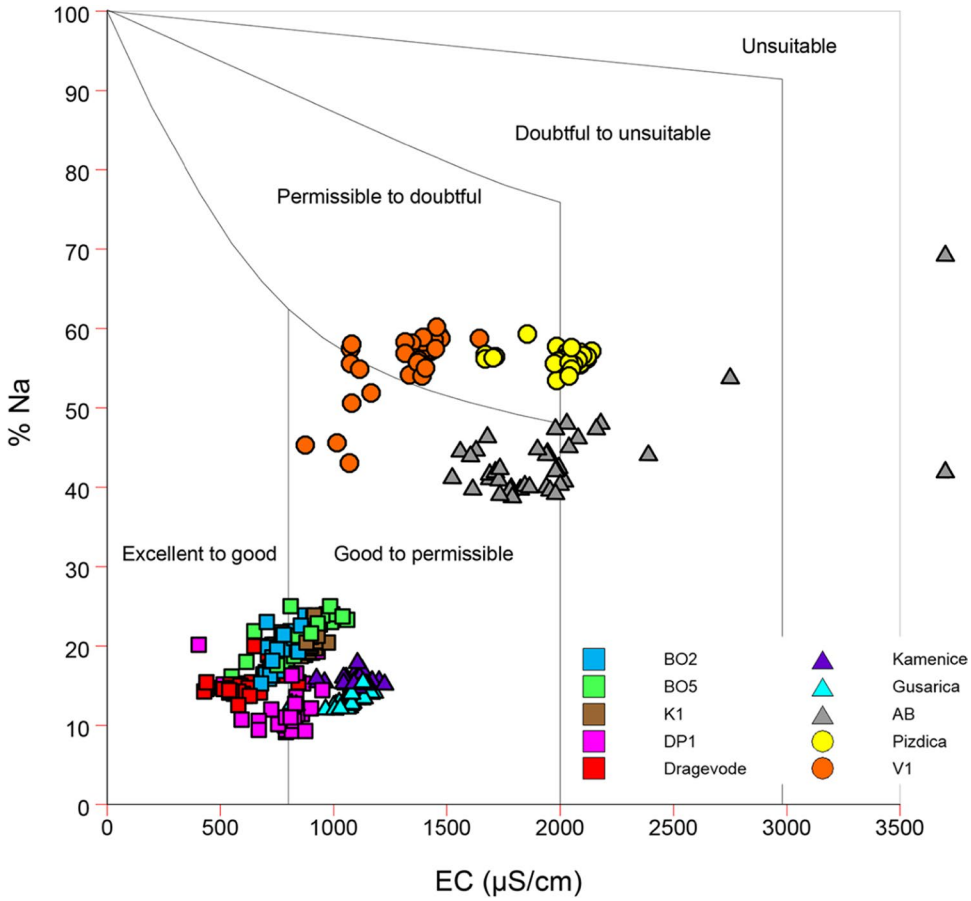

Fig. 14 Wilcox diagram of groundwater samples

user conflicts as the intensity and frequency of droughts on the island increase.

Although the water supply system on the island of Vis meets most of the annual demand, the problem of fivefold summer demand still needs to be solved. Currently, the maximum pumping limit is imposed by the engineering limitation (i.e., lack of pumping capacity) rather than salinization hazard. Terzić et al. (2022) suggested the possibility of drilling additional wells and increasing the pumping capacity of the Korita well field. However, such a measure should be accompanied by the development of an early warning system for seawater intrusion, ideally situated along the fault zones toward the E and N–NE, as these are the directions of the most likely advance of seawater–freshwater interface (Terzić et al. 2022). If the primary source of chlorides is seawater upconing below the Korita well field rather than the preferential intrusion via faults, high-resolution data sets of groundwater levels and EC should be utilized to provide sufficient evidence. In terms of water management, several measures could be undertaken to reduce the risk of water shortage during the peak summer months, such as drilling of a backup well (to bypass eventual malfunction of the existing pump/well) in the Korita well field, tightening of the existing water conservation methods, further reduction in losses from the water supply system, investigation of prospective areas for new water supply wells, and alternative water supply schemes (e.g., small desalination plant, revitalization of existing rainwater harvesting systems, and managed aquifer recharge; Patekar et al. 2022).

Conclusions

Detailed and long-term hydrochemical monitoring and analyses were done to assess the origin and processes that govern the composition and distribution of major ions in groundwater on the island of Vis. The island is autonomous in water supply, and groundwater resources, recharged solely by precipitation, face high seasonal stress due to an intensive pumping regime, low recharge, and potential quality degradation. In a long-term perspective, local groundwater resources will be affected by adverse effects of climate change through an increase in air temperature, seasonal redistribution of precipitation, and an increase in climate extremes, all of which will influence local evapotranspiration, infiltration, and groundwater recharge. During a 4-year investigation period, 376 groundwater

samples from borewells, dug wells, and natural springs were collected and analyzed.

Three distinctive hydrochemical facies were indicated based on Piper and Schoeller diagrams: i) Ca–HCO_3 group, ii) mixed group, and iii) Na–Cl group. Given the abundance of Ca, Mg, and HCO_3 in all three groups and local geological settings, carbonate dissolution plays a crucial role in defining the chemical composition of the local groundwater. Dolomite is the prevailing lithology along the western coast, while a mixed dissolution of limestone and dolomite occurs within the island's interior and along the eastern coast. In the western part of the island, higher SO_4 concentrations in groundwater are derived from gypsum and anhydrite dissolution associated with the VSE complex of the Komiža bay. The analyses of $\delta^{34}S$ and $\delta^{18}O$ from SO_4 confirm the relatively narrow extent and localized effect of the VSE zone in the western part of the island, whereas, in the central and eastern parts, the primary sources of SO_4 are atmospheric deposition and marine contribution. A minor effect of dedolomitization, associated with gypsum and dolomite dissolution, was observed in the western part of the island.

Variations in Na and Cl concentrations exist across all hydrochemical groups. This likely reflects the influence of multiple factors, including mixing of seawater and freshwater, infiltration of marine aerosols, and atmospheric deposition. The highest concentrations of Na and Cl are observed in coastal wells and springs, where seawater penetrates highly fractured and karstified rock mass, forming a transitional mixing zone between fresh groundwater and seawater. The main aquifer from which the majority of high-quality groundwater is abstracted (i.e., aquifer tapped by the Korita well field) is an unconfined, fractured and karstified carbonate aquifer, ideally situated in the central part of the island, where it is protected from significant seawater intrusion by hydrogeological barriers from the west (impervious VSE complex of the Komiža bay) and the south (infilled rock mass of very low permeability below karst poljes). Still, chloride concentrations up to 155 mg/l indicate that a small fraction of seawater still reaches this aquifer through the main E–W fault (Komiža-Vis fault) or lower-order NE–SW faults, or as a consequence of seawater upconing, despite the presence of relatively watertight dolomitic intrabed in the base of this aquifer. The low percentage of seawater in the mixture ($< 1\%$ in Ca–HCO_3 group and $< 2\%$ in Na–Cl and mixed group) indicates that seawater intrusion is not too extensive even during prolonged dry periods, implying favorable and balanced hydrostatic regime with relatively small but sufficient groundwater reserves of the island's aquifers. Moreover, seawater intrusion promotes the process of reverse ion exchange, where excess Na from groundwater is exchanged with Ca and Mg from the aquifer matrix.

The authors hope that this study will serve as a knowledge basis and facilitate further development of local water management scheme, focusing on sustainability, safety, and long-term resilience. Several open issues remain following this study, and further research should aim to perform continuous monitoring of EC and groundwater levels using data loggers, sampling of precipitation, 3D reconstruction and numerical modeling, as well as cost–benefit analyses of alternative solutions that support local water supply (e.g., small desalination plant, revitalization of rainwater harvesting systems, or managed aquifer recharge).

Acknowledgements Presented research was done in the scope of the internal research project SIS-VIS at the Croatian Geological Survey, funded by the National Recovery and Resilience Plan 2021–2026 of the European Union – NextGenerationEU, and monitored by the Ministry of Science and Education of the Republic of Croatia, and DEEPWATER-CE project through Interreg-CE program funded by the European Regional Development Fund (ERDF).

Author contributions Conceptualization was done by Matko Patekar, Staša Borović; Data curation: Matko Patekar, Josip Terzić, and Staša Borović; formal analysis was done by Matko Patekar and Maja Briški; funding acquisition was done by Josip Terzić and Staša Borović; investigation was done by Matko Patekar, Maja Briški, Josip Terzić, Zoran Nakić, and Staša Borović; methodology was done by Josip Terzić and Zoran Nakić; Resources were done by Josip Terzić and Staša Borović; visualization was done by Matko Patekar; supervision was done by Zoran Nakić and Staša Borović; writing—original draft were done by Matko Patekar; writing—review and editing were done by Matko Patekar, Maja Briški, Josip Terzić, Zoran Nakić, and Staša Borović.

Funding The authors received no specific funding for this work.

Declarations

Conflict of interest On behalf of all authors, the corresponding author states that there is no conflict of interest.

References

Abu-alnaeem MF, Yusoff I, Tham FN, Alias Y (2018) Assessment of groundwater salinity and quality in Gaza coastal aquifer, Gaza Strip, Palestine: an integrated statistical, geostatistical

and hydrogeochemical approaches study. Sci Total Environ 615:972–989. https://doi.org/10.1016/j.scitotenv.2017.09.320
Aguilera H, Murillo JM (2009) The effect of possible climate change on natural groundwater recharge based on a simple model: a study of four karstic aquifers in SE Spain. Environ Geol 57:963–974. https://doi.org/10.1007/s00254-008-1381-2
Al Haj R, Merheb M, Halwani J, Ouddane B (2023) Hydrogeochemical characteristics of groundwater in the Mediterranean region: a meta-analysis. Phys Chem Earth. https://doi.org/10.1016/j.pce.2022.103351
Al-Ahmadi ME (2013) Hydrochemical characterization of groundwater in wadi Sayyah, Western Saudi Arabia. Appl Water Sci 3:721–732. https://doi.org/10.1007/s13201-013-0118-x
Antonellini M, Mollema P, Giambastiani B, Bishop K, Caruso L, Minchio A, Pellegrini L, Sabia M, Ulazzi Gabbianelli E (2008) Salt water intrusion in the coastal aquifer of the southern Po Plain, Italy. Hydrogeol J 16:1541–1556. https://doi.org/10.1007/s10040-008-0319-9
Appelo CAJ, Postma D (2005) Geochemistry, groundwater and pollution, 2nd edn. CRC Press, London
Argamasilla M, Barberá JA, Andreo B (2017) Factors controlling groundwater salinization and hydrogeochemical processes in coastal aquifers from southern Spain. Stoten 580:50–68. https://doi.org/10.1016/j.scitotenv.2016.11.173
Bartolini G, di Stefano V, Maracchi G, Orlandini S (2012) Mediterranean warming is especially due to summer season–evidences from Tuscany (central Italy). Theor Appl Climatol 107:279–295. https://doi.org/10.1007/s00704-011-0481-1
Behera AK, Chakrapani GJ, Kumar S, Rai N (2019) Identification of seawater intrusion signatures through geochemical evolution of groundwater: a case study based on coastal region of the Mahanadi delta, Bay of Bengal, India. Nat Hazards 97:1209–1230. https://doi.org/10.1007/s11069-019-03700-6
Bisselink B, Bernhard J, Gelati E, Adamovic M, Guenther S, Mentaschi L, De Roo A (2018) Impact of a changing climate, land use, and water usage on Europe's water resources. Publications Office of the European Union, Luxembourg
Bonacci O (2001) Monthly and annual effective infiltration coefficients in Dinaric karst: example of the Gradole karst spring catchment. Hydrol Sci J 46:287–299. https://doi.org/10.1080/02626660109492822
Bonacci O, Bonacci D, Patekar M, Pola M (2021) Increasing trends in air and sea surface temperature in the Central Adriatic sea (Croatia). J Mar Sci Eng 9(4):358. https://doi.org/10.3390/jmse9040358
Bonacci O, Patekar M, Pola M, Roje-Bonacci T (2020) Analyses of climate variations at four meteorological stations on remote islands in the croatian part of the Adriatic sea. Atmosphere 11(10):1044. https://doi.org/10.3390/atmos11101044
Borović S, Terzić J, Pola M (2019) Groundwater Quality on the Adriatic Karst Island of Mljet (Croatia) and Its Implication on Water Supply. Geofluids. https://doi.org/10.1155/2019/5142712
Branković Č, Güttler I, Gajić-Čapka M (2013) Evaluating climate change at the Croatian Adriatic from observations and regional climate models' simulations. Clim Dyn 41:2353–2373. https://doi.org/10.1007/s00382-012-1646-z
Capaccioni B, Didero M, Paletta C, Salvadori P (2001) Hydrogeochemistry of groundwater from carbonate formations with basal gypsiferous layers: an example from the Mt Catria-Mt Nerone ridge (Northern Appennines, Italy). J Hydrol 253(1–4):14–26. https://doi.org/10.1016/S0022-1694(01)00480-2
Cappucci S, De Cassan M, Grillini M, Proposito M, Screpanti A (2020) Multi-source water characterisation for water supply and management strategies on a small Mediterranean island. Hydrogeol J 28:1155–1171. https://doi.org/10.1007/s10040-020-02138-6
CBS (2021) Croatian Bureau of Statistics. Population Census of 2021. Available online: https://podaci.dzs.hr/hr/podaci/stanovnistvo/popis-stanovnistva (accessed on 14 January 2024)
Colombani N, Cuoco E, Mastrocicco M (2017) Origin and pattern of salinization in the Holocene aquifer of the southern Po Delta (NE Italy). J Geochem Explor 175:130–137. https://doi.org/10.1016/j.gexplo.2017.01.011
European Commision (2020) The drinking water directive. official journal of the european union. Available online: https://eur-lex.europa.eu/legal-content/EN/TXT/PDF/?uri=CELEX:32020L2184 Accessed on 5 March 2024
Crnolatac I (1953) Geologija otoka Visa [Geology of the island of Vis]. Geološki Vjesnik 33:45–62
Cudennec C, Leduc C, Koutsoyiannis D (2007) Dryland hydrology in Mediterranean regions—a review. Hydro Sci J 52(6):1077–1087. https://doi.org/10.1623/hysj.52.6.1077
Duplančić Leder T, Ujević T, Čala M (2004) Coastline lenghts and areas of islands in the Croatian part of the Adriatic Sea determined from the topographic maps at the scale of 1:25 000. Geoadria 9(1):5–32. https://doi.org/10.15291/geoadria.127
Fernández-Ortega J, Barberá JA, Andreo B (2024) Real-time karst groundwater monitoring and bacterial analysis as early warning strategies for drinking water supply contamination. Sci Total Environ 912:169539. https://doi.org/10.1016/j.scitotenv.2023.169539
Ford D, Williams P (2007) Karst hydrogeology and geomorphology. John Wiley & Sons Ltd, New York
Frondini F (2008) Geochemistry of regional aquifer systems hosted by carbonate-evaporite formations in Umbria and southern Tuscany (central Italy). Appl Geochem 23(8):2091–2104. https://doi.org/10.1016/j.apgeochem.2008.05.001
Gajić-Čapka MA, Zaninović KS. Climate of Croatia. In: Zaninović K (ed) Climate atlas of Croatia 1961–1990, 1971–2000. Croatian Meteorological and Hydrological Service, Zagreb. https://klima.hr/razno/publikacije/klimatski_atlas_hrvatske.pdf Accessed on 4 February 2024
García-Ruiz JM, López-Moreno JI, Vicente-Serrano SM, Lasanta Martínez T, Beguería S (2011) Mediterranean water resources in a global change scenario. Earth-Sci Rev 105(3–4):121–139
Ghabayen MS, McKee M, Kemblowski M (2006) Ionic and isotopic ratios for identification of salinity sources and missing data in the Gaza aquifer. J Hydrol 318(1–4):360–373. https://doi.org/10.1016/j.jhydrol.2005.06.041
Goldscheider N, Andreo B (2007) The geological and geomorphological framework. In: Goldscheider N, Williams P (eds) Methods in karst hydrogeology. Taylor & Francis, London
Hamma B, Alodah A, Bouaicha F, Bekkouche MF, Barkat A, Hussein EE (2024) Hydrochemical assessment of groundwater using multivariate statistical methods and water quality indices (WQIs). Appl Water Sci 14:33. https://doi.org/10.1007/s13201-023-02084-0
IAEA (2005) Isotopic composition of precipitation in the mediterranean basin in relation to air circulation patterns and climate. TECDOC Series No. 1453, IAEA, Vienna, pp. 223
IAEA/WMO (2006) Global Network of Isotopes in Precipitation. The GNIP database. Available online: https://www.iaea.org/services/networks/gnip Accessed on 15 March 2024
Ismail AH, Shareef MA, Hassan G, Alatar FM (2023) Hydrochemistry and water quality of shallow groundwater in the Tikrit area of Salah Al Din Province. Iraq Appl Water Sci 13:197. https://doi.org/10.1007/s13201-023-02008-y
Kim Y, Kwang-Sik L, Dong-Chan K, Dae-Ha L, Seung-Gu L, Won-Bae P, Gi-Won K, Nam-Chil W (2003) Hydrogeochemical and isotopic evidence of groundwater salinization in a coastal aquifer: a case study in Jeju volcanic island. Korea J Hydrol

270(3–4):282–294. https://doi.org/10.1016/S0022-1694(02)00307-4
Korbar T, Belak M, Fuček L, Husinec A, Oštrić N, Palenik D, Vlahović I (2012) Basic geological map of the Republic of Croatia 1:50.000. Sheets Vis 3 and Biševo 1 with part of the sheet Vis 4 and islands Sv Andrija, Brusnik, Jabuka and Palagruža. Croatian Geological Survey, Zagreb
Krishna Kumar S, Bharani R, Magesh NS et al (2014) Hydrogeochemistry and groundwater quality appraisal of part of south Chennai coastal aquifers, Tamil Nadu, India using WQI and fuzzy logic method. Appl Water Sci 4:341–350. https://doi.org/10.1007/s13201-013-0148-4
Krklec K, Lozić S, Perica D (2012) Neke značajke klime otoka Visa [Some Climate Features of the Island of Vis – in Croatia]. Naše More 59(3–4):148–160
Krklec K, Lozić S, Šiljeg A, Perica D, Šiljeg S (2015) Morphogenesis of karst poljes on Vis Island, Croatia. J Cent Eur Agric 16(2):99–116. https://doi.org/10.5513/JCEA01/16.2.1595
Leduc C, Pulido-Bosch A, Remini B (2017) Anthropization of groundwater resources in the Mediterranean region: processes and challenges. Hydrogeol J 25:1529–1547. https://doi.org/10.1007/s10040-017-1572-6
López-Chicano M, Bouamama M, Vallejos A, Pulido-Bosch A (2001) Factors which determine the hydrogeochemical behaviour of karstic springs. A case study from the Betic Cordilleras Spain. Appl Geochem 16(9–10):1179–1192. https://doi.org/10.1016/S0883-2927(01)00012-9
Luterbacher J, Xoplaki E, Casty C, Wanner H, Pauling A, Küttel M, Rutishauser T, Brönnimann S et al (2006) Chapter 1 Mediterranean climate variability over the last centuries: a review. In: Lionello P et al (eds) Developments in earth and environmental sciences. Elsevier, Amsterdam
Mahlknecht J, Merchán D, Rosner M, Meixner A, Ledesma-Ruiz R (2017) Assessing seawater intrusion in an arid coastal aquifer under high anthropogenic influence using major constituents, Sr and B isotopes in groundwater. Sci Total Environ 587–588:282–295. https://doi.org/10.1016/j.scitotenv.2017.02.137
Massuel S, Riaux J (2017) Groundwater overexploitation: why is the red flag waved? Case study on the Kairouan plain aquifer (central Tunisia). Hydrogeol J 25:1607–1620. https://doi.org/10.1007/s10040-017-1568-2
Mazor E (2004) Chemical and isotopic groundwater hydrology. Marcel Dekker, New York
Mercado A (1985) The use of hydrogeochemical patterns in carbonate sand and sandstone aquifers to identify intrusion and flushing of saline water. Groundwater 23(5):635–645. https://doi.org/10.1111/j.1745-6584.1985.tb01512.x
Ministry of Health and Social Care of Croatia (MHSS) (2008) Ordinance on drinking water quality. Official Gazette of the Republic of Croatia, 47: 1593. Available online: https://narodne-novine.nn.hr/clanci/sluzbeni/2008_04_47_1593.html Accessed on 6 March 2024
Mongelli G, Monni S, Oggiano G, Paternoster M, Sinisi R (2013) Tracing groundwater salinization processes in coastal aquifers: a hydrogeochemical and isotopic approach in the Na-Cl brackish waters of northwestern Sardinia. Italy Hydrol Earth Syst Sci 17:2917–2928. https://doi.org/10.5194/hess-17-2917-2013
Mora A, Mahlknecht J, Ledesma-Ruiz R, Sanford W, Lesser L (2020) Dynamics of major and trace elements during seawater intrusion in a coastal sedimentary aquifer impacted by anthropogenic activities. J Contam Hydrol 232:103653. https://doi.org/10.1016/j.jconhyd.2020.103653
Moral F, Cruz-Sanjulián JJ, Olías M (2008) Geochemical evolution of groundwater in the carbonate aquifers of Sierra de Segura (Betic Cordillera, southern Spain). J Hydrol 360(1–4):281–296. https://doi.org/10.1016/j.jhydrol.2008.07.012
Mussa KR, Mjemah IC (2023) Using hydrogeochemical facies and signatures for groundwater characterization and evolution assessment in aquifers with contrasting climate and geology in Tanzania. Appl Water Sci 13:201. https://doi.org/10.1007/s13201-023-01977-4
Novak G (1940) Kolonizatorsko djelovanje Dionizija Starijeg na Jadranu [Adriatic colonization of dionis the older – in Croatian]. Serta Hoffilleriana, Zagreb
Patekar M, Bašić M, Pola M, Kosović I, Terzić J, Lucca A, Mittempergher S, Berio LR, Borović S (2022) Multidisciplinary investigations of a karst reservoir for managed aquifer recharge applications on the island of Vis (Croatia). Acque Sotterran - Ital J Groundw 11(1):37–48. https://doi.org/10.7343/as-2022-557
Patekar M, Soža M, Pola M, Nakić Z, Bašić M, Terzić J, Borović S (2023) Feasibility study of managed aquifer recharge deployment on the Island of Vis (Croatia). Sustainability 15(13):9934. https://doi.org/10.3390/su15139934
Piper AM (1944) A graphic procedure in the geochemical interpretation of water-analyses. Trans Am Geophys Union 25(6):914–928. https://doi.org/10.1029/TR025i006p00914
Plummer N, Busby J, Lee R, Hanshaw B (1990) Geochemical modeling of the madison aquifer in parts of Montana, Wyoming, and South Dakota. Water Resour Res 26(9):1981–2014. https://doi.org/10.1029/WR026i009p01981
Porowski A, Porowska D, Halas S (2019) Identification of sulfate sources and biogeochemical processes in an aquifer affected by Peatland: Insights from Monitoring the isotopic composition of groundwater sulfate in Kampinos national park. Poland Water 11:1388. https://doi.org/10.3390/w11071388
Reale M, Salon S, Crise A, Mosetti FR, Sannino G (2017) Unexpected covariant behavior of the aegean and ionian seas in the period 1987–2008 by means of a nondimensional sea surface height index. J Geophys Res Oceans 122(10):8020–8033. https://doi.org/10.1002/2017JC012983
Samaniego L, Thober S, Kumar R, Wanders N, Rakovec O, Pan M, Zink M, Sheffield J, Wood EF, Marx A (2018) Anthropogenic warming exacerbates European soil moisture droughts. Nature Clim Change 8:421–426. https://doi.org/10.1038/s41558-018-0138-5
Schoeller H (1962) Les eaux souterraines: Hydrologie dynamique et statique Comptes rendus critiques. Hydrogéologie en chamber, Paris
Schoeller H (1965) Qualitative evaluation of groundwater resources. In: Schoeller H (ed) Methods and techniques of groundwater investigation and development. Water resources series No 33. UNESCO, Paris
Serianz L, Cerar S, Šraj M (2020) Hydrogeochemical characterization and determination of natural background levels (NBL) in groundwater within the main lithological units in Slovenia. Environ Earth Sci 79:373
Simler R (2012). Software Diagrammes, V6.72. Laboratoire d'Hydrologie d'Avignon, Université d'Avignon et pays du Vaucluse, Avignon, France. http://www.lha.univ-avignon.fr
Skevin-Sović J, Djuričić V, Kosanović C (2012) major ions wet deposition and trends during the last decade on the Eastern Adriatic Coast. Air Polution XX 157(11):339–349. https://doi.org/10.2495/AIR120301
Sun H, Bian K, Wang T, Jin Z, Niu Z (2023) Hydrogeochemical characteristics and genetic analysis of Karst groundwater in the Fengfeng mining area. Water 15(23):4049. https://doi.org/10.3390/w15234049
Tanvir Rahman MATM, Saadat AHM, Islam MS et al (2017) Groundwater characterization and selection of suitable water type for irrigation in the western region of Bangladesh. Appl Water Sci 7:233–243. https://doi.org/10.1007/s13201-014-0239-x

Terzic J (2004) Hidrogeološki odnosi na krškim otocima-primjer otoka Visa [Hydrogeological relations on karst island – example of the island of Vis]. Min-Geol-Pet Eng Bull 16(1):47–58

Terzić J, Frangen T, Borović S, Reberski JL, Patekar M (2022) Hydrogeological assessment and modified conceptual model of a dinaric Karst Island Aquifer. Water 14(3):404. https://doi.org/10.3390/w14030404

Terzić J, Peh Z, Marković T (2010) Hydrochemical properties of transition zone between fresh groundwater and seawater in karst environment of the Adriatic islands, Croatia. Environ Earth Sci 59:1629–1642. https://doi.org/10.1007/s12665-009-0146-x

Tiwari AK, Pisciotta A, De Maio M (2019) Evaluation of groundwater salinization and pollution level on Favignana Island. Italy Environ Pollut 249:969–981. https://doi.org/10.1016/j.envpol.2019.03.016

Tramblay Y, Llasat MC, Randin C, Coppola E (2020) Climate change impacts on water resources in the Mediterranean. Reg Environ Change 20:83. https://doi.org/10.1007/s10113-020-01665-y

Vlahović I, Tišljar J, Velić I, Matičec D (2005) Evolution of the Adriatic Carbonate Platform: palaeogeography, main events and depositional dynamics. Palaeogeogr Palaeoclimatol Palaeoecol 220(3–4):333–360. https://doi.org/10.1016/j.palaeo.2005.01.011

Vucinic L, O'Connel D, Dubber D, Coxon C, Gill L (2023) Multiple fluorescence approaches to identify rapid changes in microbial indicators at karst springs. J Contam Hydrol 254:104129. https://doi.org/10.1016/j.jconhyd.2022.104129

Wali SU, Alias N, Harun SB (2020) Quality reassessment using water quality indices and hydrochemistry of groundwater from the basement complex section of Kaduna Basin. NW Nigeria SN Appl Sci 2:1742. https://doi.org/10.1007/s42452-020-03536-x

WHO (1997) Guidelines for drinking-water quality (2nd edition) – Volume 3: Surveillance and control of community supplies. WHO, Geneva. Available online: https://iris.who.int/bitstream/handle/10665/42002/9241545038.pdf?sequence=1 Accessed on 5 March 2024

Zaidi FK, Nazzal Y, Jafri MK, Naeem M, Ahmed I (2015) Reverse ion exchange as a major process controlling the groundwater chemistry in an arid environment: a case study from northwestern Saudi Arabia. Environ Monit Assess 187(10):607. https://doi.org/10.1007/s10661-015-4828-4

Zhang B, Zhao D, Zhou P, Qu S, Liao F, Wang G (2020) Hydrochemical characteristics of groundwater and dominant water-rock interactions in the Delingha area, Qaidam Basin. Northwest China Water 12(3):836. https://doi.org/10.3390/w12030836

Zhang R, Zhang B, Guo Y, Kong X, Li Y, Liu Y, Chen L, Gong Q (2023) Replenishment impacts on hydrogeochemistry and water quality in the Hutuo River Plain. Water 15(19):3326. https://doi.org/10.3390/w15193326